The Propagation of Auxin Waves and Wave trains

Philipp Moser

22-10-2020

Supervisors:
Dr H.J. Hupkes
Prof. Dr. R.M.H. Merks
Prof. Dr. T. Schmidt

Bachelor Thesis

Mathematical Institude
Leiden University

Contents

Abstract

Many things remain unknown about the functioning of Auxin in plant development of growth. We evaluate two models regarding Auxin propagation and investigate whether they allow for the formation of Auxin pulses. We numerically uncover the existence of families of small-amplitude traveling pulses and theoretically analyze their leading order behaviour.

Chapter 1

Introduction

Modern data indicates that approximately 98% of all oxygen is produced by plants and plant-like growths. Given this figure, the growth and development of plants is a very important matter. Why do plants grow in different shapes and sizes? Why is one leaf larger than the other? Why do some leaves have holes? What are the important factors in determining the morphology of a plant? [1]

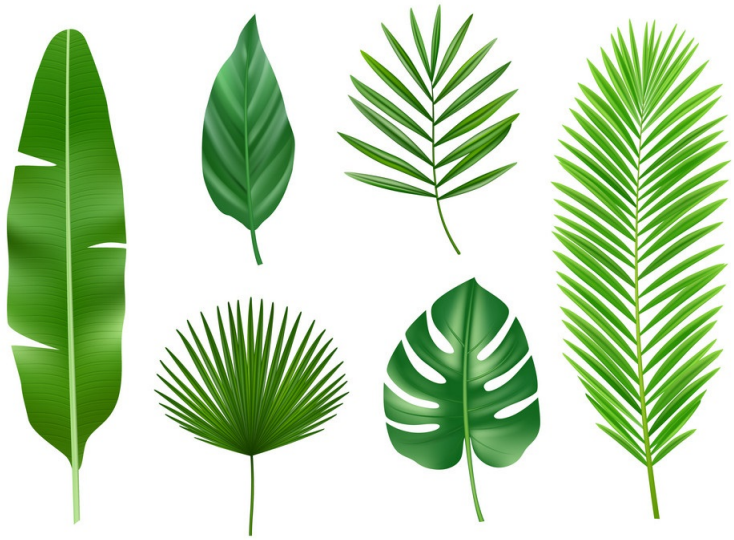

Figure 1.1: Varying plants with unique leaves. Figure adapted from https://www.vectorstock.com/royalty-free-vector/tropical-plants-exotic-eco-nature-green-leaves-vector-23992912

Ongoing research

Despite the importance of these questions, we know surprisingly little about plant growth. As in humans, plant growth is governed by a multitude of hormones. One of the few things that we do know, is that a hormone called Auxin plays an important factor in growth and organ development [17], as well as "endocytosis, cell polarity, and cell cycle control" [12], and "... the location of the quiescent centre and surrounding stem cells" [13]. In spite of the fact that there have been "remarkable breakthroughs in understanding [Auxin] production, transport, and perception" [16], we still know very little about the actual molecular functioning of the hormone. Ever since the canalization hypothesis was proposed by Tsvi Sachs [11], much research has been going on. One article, for example, explored how Auxin can be used to improve the yield of crops, such as rice [15]. Another important aspect of Auxin, is how it affects the growth and development of vascular patterning. It is believed that this is governed by "a self-organizing pattern of auxin transport – canalization" [4]. A model to study the vascular pattern formation is "..the process of leaf vascularization in Arabidopsis" [5].

One important area of research, is the transportation of Auxin. Using radioactive Auxin, one pair of researchers found that "Auxin molecules are most likely transported by anon-covalent mechanism" [8]. Specifically, several articles found that a molecule named PIN1 played an important role in transport [6] [7]. Based on this discovery, researchers have begun computationally modelling the transportation of Auxin [10].

While the precise mechanism by which the presence of Auxin in a cell stimulates said cell to develop is quite fascinating, in this paper I will be discussing the propagation and movement of auxin concentrations.

Proposed models

Little is known about the details of Auxin transport. Several different models have been proposed to describe the movement of auxin, however as of yet there is no definitive answer.

One important hypothesis was proposed in 1969 by Tsvi Sachs: the canalization hypothesis [11]. According to this hypothesis, a positive feedback loop between the flux of Auxin, and a cell's ability to transport Auxin leads to the hormone being channeled. These channels resemble "the way that streaming water carves out a river system" [9].

Based on said hypothesis, we will consider two similar models. One model was proposed by Roeland Merks et al [9], the other by Henry Allen and Mariya Ptashnyk [3]. Both models assume that Auxin transport is facilitated through the polarized version of a molecule called PIN1; a molecule that attaches itself to the cell wall, and effectively pulls Auxin through. The central difference between the models is the mechanism by which PIN1 polarizes: in the model by Merks, polarization is determined by the Auxin concentration in neighbouring cells. In the model by Allen however, the direction fo the Auxin flow is the

determining factor.

Traveling Waves

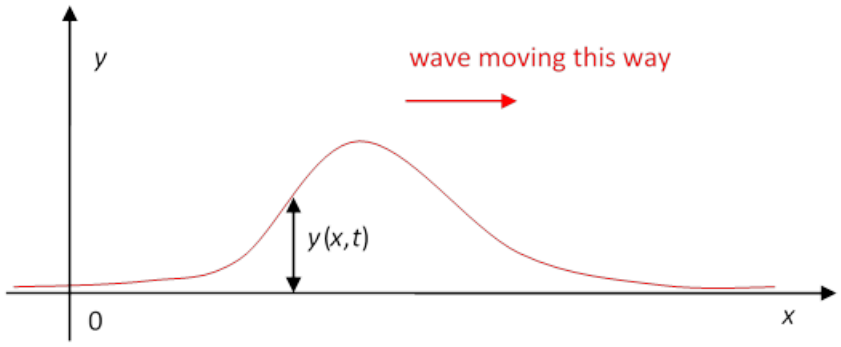

Figure 1.2: A still image of a traveling wave.

An important type of equation to study general propagation phenomena is the reaction-diffusion-equation [2]:

$$\frac{du}{dt} = \nabla \cdot (D\nabla u) + R(u, \nabla u).$$

Here, $u(x,t)$ describes the concentration of the particle we're interested in, and D is a diffusion coefficient. The first term on the right hand side represents diffusion, while the second term represents active transport (or creation and decay). These equations are frequently used in chemistry, ecology, physics and physiology to describe the changing concentration of a quantity, given that this change is both diffusive, as well as through some sort of reaction. We note that this will neatly fit the equation of Auxin we will deal with: we will have a diffusive term on account of differences in concentration, and a term corresponding to Auxin displacement via PIN1, which we can locally interpret as creation or destruction of Auxin.

While our findings may differ, an example to guide our thinking is the "Fisher Kolmogorov Petrovsky-Piscounov" (or FKPP) equation. In this case, one chooses $R(u) = u(1-u)$. We look at a one-dimensional version. Furthermore, if we set $D = 1$, we find the equation

$$\frac{du}{dt} = \frac{d^2u}{dx^2} + ru(1-u).$$

A verifiable solution to this equation is $u(x,t) = \phi(x - ct)$, with $c \geq 2$, ϕ

differentiable, and $D\phi'' + c\phi' + r\phi(1-\phi) = 0$. For example, we have

$$\phi(x-ct) = \frac{1}{(1+Ce^{\mp\frac{(x-ct)}{\sqrt{6}}})^2}$$

in the case of $c = \frac{5}{\sqrt{6}}$. We note that C is a phase, which we may pick arbitrarily.

Solutions of this form are called traveling waves; these waves have a fixed rigid profile, which moves through space as time passes, and as such have both time and space as arguments. Specifically, the arguments may be combined as $x - ct$: we see that for larger t, x needs to be larger to get the same argument, which matches movement to the right in figure 1.2.

In the models I will discuss, I will deal with a discretized set of cells Λ; therefore, we also need a discretized version of the FKPP equation. On a final note, since we will deal with two different models, we will call the active transport term $R_{discrete}$, and leave it undefined for now. We expect the equation to look like this:

$$\frac{du(i,t)}{dt} = (u(i-1,t)+u(i+1,t)-2u(i,t))+R_{discrete}(u(i,t),u(i-1,t),u(i+1,t)).$$

In this equation we have $i \in \Lambda$, our discrete set of cells. As a result, we also expect a spatially discretized traveling wave solution. We assume this solution to be of the form

$$u(i,t) = \phi(i-ct).$$

Again we have $i \in \Lambda$.

The aim of the thesis

In this thesis, we explore the differences and similarities between these two models. The first model, the one proposed by Merks, predicts that with a constant influx of Auxin, at first the Auxin will stockpile, and after reaching a certain threshold it will travel across the cells, after which the process repeats. The resulting pattern will look like 'wave trains'. We investigated whether the same behaviour occurs in the model by Allen and Mariya Ptashnyk, or whether something radically different happens. Often, we will reference the work done by Jelle van der Voort in his thesis [14], as he explored the former model.

Structure of the thesis

First, we will introduce the model we will base ourselves on; the model by Roeland Merks. Subsequently, we will introduce the adaptations we made based on the model by Allen. After having fully introduced the model, I will start with a numerical solution, obtained by using MATLAB. From these simulations, we will deduce the correlation between several of the solutions properties. Using these correlations, I will attempt to find a leading order solution of the equations of motion. Having done all this, I will numerically evaluate the differences between the models, with regard to the presence of 'wave trains'.

Chapter 2

Model description

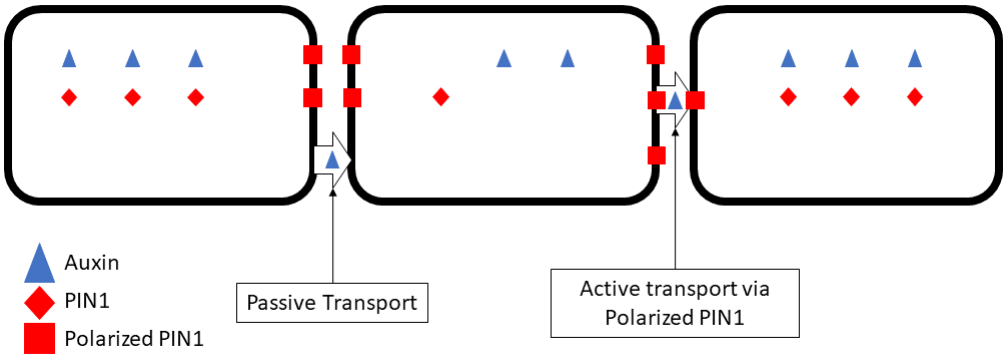

Figure 2.1: Schematic representation of Auxin transport, both through diffusion and through polarized PIN1. Note that Auxin moves from cell to cell, while PIN1 does not.

2.1 Common structure

To understand the dynamics of Auxin, I will be basing myself on the model created by Merks et al [9], and the model created by Allen et al [3]. The models are fairly alike, so we will elaborate on the similarities, before going into detail on the differences.

According to both models, active Auxin transport is facilitated by a molecule named PIN1, which is created under influence of Auxin. More specifically, active transport is facilitated by a polarized version PIN1. We note that this polarization is always towards another neighboring cell. It is this polarization where the models differ. Before going into the specifics, we will introduce the

variables we use:

- $A_i(t)$ is the amount of Auxin in cell i.
- $P_i(t)$ is the amount of PIN1 in cell i.
- $P_{ij}(t)$ is the amount of polarized PIN1 in cell i that is polarized towards cell j.

Here we take $i \in \Lambda$, with Λ our set of cells. Furthermore, we take $j \in \mathcal{N}_i$, where $\mathcal{N}_i \subset \Lambda$ is the set of all cells adjacent to cell i.

2.1.1 Auxin dynamics

The transfer of auxin is facilitated both by a diffusive part, and active transport by polarised PIN1. We will write

$$\frac{dA_i(t)}{dt} = F_{\text{act}} + F_{\text{diff}}.$$

The active part is determined by the amount of polarized PIN1. Since no active transport can take place without Auxin, and the polarized PIN1 will eventually be 'saturated', Merks introduced a normalized term to account for this, which we will call NORM:

$$\text{NORM}_j = \frac{A_j(t)}{k_a + A_j(t)}.$$

Of course, the amount of PIN1 is also relevant. When we multiply this with the polarized PIN1 concentration, and account for transport back from an adjacent cell, the active auxin flux between two cells i, j looks like

$$\text{FLUX}_{ij} = P_{ji}(t)\text{NORM}_j - P_{ij}(t)\text{NORM}_i.$$

Finally, taking all surrounding cells into consideration and applying an overall coëfficiënt, the active transport of Auxin becomes

$$F_{\text{act}} = T_{act} \sum_{j \in \mathcal{N}_i} \text{FLUX}_{ij}.$$

The diffusive part is determined entirely by the length of shared border between cells, L_{ij}, and the 'auxin gradient' $A_j(t) - A_i(t)$:

$$F_{\text{diff}} = T_{diff} \sum_{j \in \mathcal{N}_i} L_{ij}(A_j(t) - A_i(t)).$$

Ultimately, the differential equation describing auxin is as follows:

$$\frac{dA_i(t)}{dt} = T_{act} \sum_{j \in \mathcal{N}_i} \left(P_{ji}(t)\frac{A_j(t)}{k_a + A_j(t)} - P_{ij}(t)\frac{A_i(t)}{k_a + A_i(t)}\right) + T_{diff} \sum_{j \in \mathcal{N}_i} L_{ij}(A_j(t) - A_i(t)). \quad (2.1)$$

2.1.2 PIN1 dynamics

In the dynamics of PIN1, four different terms can be identified: PIN1 polarization, polarized PIN1 depolarization, PIN1 production and PIN1 decay. As stated before, we will leave the polarization term undefined for now. For the time being, we will write it as $\mathcal{P}_{i,j}(t)$. We can thus write:

$$\frac{dP_i(t)}{dt} = -\sum_{j\in\mathcal{N}_i} \mathcal{P}_{i,j}(t) + \text{Depolarization}_i + \text{Production}_i - \text{Decay}_i.$$

In this definition i is the cell in which PIN1 is being polarized, and j is the cell in which direction it is polarized.

Depolarization is assumed to only be affected by the presence of polarized PIN1:

$$\text{Depolarization}_i = k_2 \sum_{j\in\mathcal{N}_i} P_{ij}(t).$$

As stated before, PIN1 is taken to be produced under influence of Auxin. Similarly, decay is only determined by the concentration of PIN1. Thus,production and decay are modeled by

$$\text{Production}_i - \text{Decay}_i = \alpha A_i(t) - \delta P_i(t).$$

Taking these terms together, we get the full equation for PIN1:

$$\frac{dP_i(t)}{dt} = -\sum_{j\in\mathcal{N}_i} \mathcal{P}_{i,j}(t) + k_2 \sum_{j\in\mathcal{N}_i} P_{ij}(t) + \alpha A_i(t) - \delta P_i(t). \tag{2.2}$$

2.1.3 Polarized PIN1 dynamics

Polarized PIN1 is assumed to neither decay nor be produced, except through the polarization and depolarization. Evidently, these terms are the same as in the equation above, but with signs switched:

$$\frac{dP_{ij}(t)}{dt} = \mathcal{P}_{i,j}(t) - k_2 P_{ij}(t) \tag{2.3}$$

2.1.4 The Polarization model by Merks

Having properly established most of the equations, we can get into the differences. The model by Merks posits that the Auxin concentration in neighboring cells is the dominating factor in the polarization of PIN1.

Evidently, polarization can only occur if both Auxin and PIN1 are present; furthermore, the process cannot exceed a certain rate, so we have to normalize. We expect $\mathcal{P}_{i,j}$ to look like

$$\mathcal{P}_{i,j} = k_1 \frac{R \cdot A_j(t)}{k_R + A_j(t)} \frac{P_i(t)}{k_m + P_i(t)}.$$

In this statement, R, k_1, k_R, k_m are constants. We see that for $A_j = 0$ or $P_i = 0$, no polarization will take place, while for $A_j \to \infty$ and $P_i \to \infty$ it will approach $k_1 R$. Using this term, we find that (2.3) becomes

$$\frac{dP_{ij}(t)}{dt} = k_1 \frac{R \cdot A_j(t)}{k_R + A_j(t)} \frac{P_i(t)}{k_m + P_i(t)} - k_2 P_{ij}(t). \tag{2.4}$$

Filling this term into (2.2) gives us the following equation:

$$\frac{dP_i(t)}{dt} = -k_1 \sum_{j \in \mathcal{N}_i} \frac{R \cdot A_j(t)}{k_R + A_j(t)} \frac{P_i(t)}{k_m + P_i(t)} + k_2 \sum_{j \in \mathcal{N}_i} P_{ij}(t) + \alpha A_i(t) - \delta P_i(t). \tag{2.5}$$

2.1.5 The modified model

A paper by Henry R. Allen and Mariya Ptashnyk [3] suggests that the flux of auxin is the determining factor of PIN1 polarization, rather than auxin concentration. The complete model introduces a sizeable amount of interactions and molecules, and therefore a considerable amount of parameters. To ensure that the model remains (somewhat) manageable, we use only the main part of the model. Specifically, we introduce a term $H(J_a^{ij})$ which governs the polarization of PIN1:

$$H(J_a^{ij}) = \frac{\frac{1}{1+e^{-h(\frac{J_a^{ij}}{\lambda} - \theta)}}}{\sum_{j \in \mathcal{N}_i} \frac{1}{1+e^{-h(\frac{J_a^{ij}}{\lambda} - \theta)}}}. \tag{2.6}$$

In this equation we defined the following:

$$J_a^{ij} = \sigma_a (A_i P_{ij} - A_j P_{ji}). \tag{2.7}$$

This quantity represents the Auxin flux from cell i to cell j, using σ_a as a parameter. We note that $H(J_a^{ij})$ is normalized, such that $\sum_{j \in \mathcal{N}_i} H(J_a^{ij}) = 1$ for any i.
This gives us the following expression for the polarization:

$$\mathcal{P}_{i,j} = \lambda P_i H(J_a^{ij}).$$

This term is inserted in equation (2.3) as follows:

$$\frac{dP_{ij}}{dt} = \lambda P_i H(J_a^{ij}) - k_2 P_{ij}. \tag{2.8}$$

Because the term replaces the term for PIN1 polarisation, it also has to be substituted in the equation for P_i:

$$\begin{aligned} \frac{dP_i(t)}{dt} &= -\sum_{j \in \mathcal{N}_i} \mathcal{P}_{i,j} + k_2 \sum_{j \in \mathcal{N}_i} P_{ij} + \alpha A_i(t) - \delta P_i(t) \\ &= -\lambda P_i(t) \sum_{j \in \mathcal{N}_i} H(J_a^{ij}) + k_2 \sum_{j \in \mathcal{N}_i} P_{ij}(t) + \alpha A_i(t) - \delta P_i(t). \end{aligned}$$

As stated before, $H(J_a^{ij})$ is normalized; therefore, summing over all neighbouring cells returns 1. Thus, the equation simplifies to

$$\frac{dP_i(t)}{dt} = -\lambda P_i(t) + k_2 \sum_{j \in \mathcal{N}_i} P_{ij}(t) + \alpha A_i(t) - \delta P_i(t). \tag{2.9}$$

2.1.6 Overview of both models

To summarize, the Auxin dynamics are given by (2.1):

$$\frac{dA_i(t)}{dt} = T_{act} \sum_{j \in \mathcal{N}_i} (P_{ji}(t) \frac{A_j(t)}{k_a + A_j(t)} - P_{ij}(t) \frac{A_i(t)}{k_a + A_i(t)}) + T_{diff} \sum_{j \in \mathcal{N}_i} L_{ij}(A_j(t) - A_i(t)).$$

In the model by Merks, PIN1-dynamics (both polarized and unpolarized) are given by (2.5) and (2.4) respectively:

$$\frac{dP_i(t)}{dt} = -k_1 \sum_{j \in \mathcal{N}_i} \frac{R \cdot A_j(t)}{k_R + A_j(t)} \frac{P_i(t)}{k_m + P_i(t)} + k_2 \sum_{j \in \mathcal{N}_i} P_{ij}(t) + \alpha A_i(t) - \delta P_i(t),$$
$$\frac{dP_{ij}(t)}{dt} = k_1 \frac{R \cdot A_j(t)}{k_R + A_j(t)} \frac{P_i(t)}{k_m + P_i(t)} - k_2 P_{ij}(t).$$

In the modified model by Allen, these equations are replaced by (2.9) and (2.8) respectively:

$$\frac{dP_i(t)}{dt} = -\lambda P_i(t) + k_2 \sum_{j \in \mathcal{N}_i} P_{ij}(t) + \alpha A_i(t) - \delta P_i(t),$$
$$\frac{dP_{ij}}{dt} = \lambda P_i(t) H(J_a^{ij}) - k_2 P_{ij}.$$

Chapter 3

Numerical analysis

To explore the behaviour of the model, we will run several simulations in MATLAB. The original model by Merks, applied in one dimension, leads to the formation of travelling waves [14]. We are interested whether the same, or perhaps a similar movement of Auxin can be found in the modified model we are exploring, as discussed in paragraph 2. We will be investigating both Auxin, as well as polarized PIN1.

3.1 Cell configuration

To study the system numerically, we will restrict ourselves to relatively simple cases. As one can imagine from the equations in the previous section ((2.1), (2.9), (2.8)), solving them for the general case of a plant quickly becomes impossible. Having to consider 3 dimensions, different cell shapes, and cells not being lined up neatly makes the system rather complex. We therefore make a number of restrictions;

- All cells are identical perfect squares with sides L
- We consider n cells, perfectly aligned in one dimension. We add an 'n+1th' cell that functions as an Auxin sink, much like the rest of a plant outside the viewed system.

This leaves us with significantly easier equations. For Auxin, the summation over all surrounding cells of cell i, is reduced to cells $i-1$ and $i+1$:

$$\begin{aligned}\frac{dA_i(t)}{dt} = T_{act}\Big(&P_{i-1,i}(t)\frac{A_{i-1}(t)}{k_a + A_{i-1}(t)} - P_{i,i-1}(t)\frac{A_i(t)}{k_a + A_i(t)} \\ &+ P_{i+1,i}(t)\frac{A_{i+1}(t)}{k_a + A_{i+1}(t)} - P_{i,i+1}(t)\frac{A_i(t)}{k_a + A_i(t)}\Big) \\ &+ T_{diff}L(A_{i-1}(t) + A_{i+1}(t) - 2A_i(t)). \quad (3.1)\end{aligned}$$

The same holds for the equation of PIN1:

$$\frac{dP_i(t)}{dt} = -\lambda P_i(t) + k_2(P_{i,i+1}(t) + P_{i,i-1}(t)) + \alpha A_i(t) - \delta P_i(t). \tag{3.2}$$

For the equation of polarized PIN1, the difference occurs (mostly) within the H-term. We remember equation (2.7):

$$J_a^{ij} = \sigma_a(A_i P_{ij} - A_j P_{ji}).$$

For the sake of simplicity, we introduce the following notation:

$$J_{i\pm} \equiv J_a^{i,i\pm1}. \tag{3.3}$$

Now, we can define the quantity

$$h_{i\pm} = \frac{1}{1 + e^{-h(\frac{J_{i\pm}}{\lambda} - \theta)}}. \tag{3.4}$$

Using these definitions, we can write $H(J_{i\pm}, J_{i\mp})$ in a more manageable form:

$$H(J_{i\pm}, J_{i\mp}) = \frac{h_{i\pm}}{h_{i+} + h_{i-}}. \tag{3.5}$$

Then, (2.8) is split into two distinct equations:

$$\frac{dP_{i,i+1}(t)}{dt} = \lambda P_i(t) \cdot \frac{h_{i+}}{h_{i+} + h_{i-}} - k_2 P_{i,i+1}(t), \tag{3.6}$$

and

$$\frac{dP_{i,i-1}(t)}{dt} = \lambda P_i(t) \cdot \frac{h_{i-}}{h_{i+} + h_{i-}} - k_2 P_{i,i-1}(t). \tag{3.7}$$

We note that (3.6) and (3.7) are two equations; one for $P_{i,i+1}$ and one for $P_{i,i-1}$. However, for simplicity (and because we will treat these variables the same way for now), we will often write them together, as seen in the previous chapter. Finally, we will denote PIN1 that is polarized to the cell on the right ($P_{i,i+1}$) as RPIN, and PIN1 that is polarized to the cell on the left ($P_{i,i-1}$) as LPIN from now on.

3.2 Additional conditions

3.2.1 Initial conditions

Having simplified our equations, we can almost start to solve the system. Before that, however, we need a few initial and boundary conditions. First off, we assume that no Auxin is present in the system, other than a set amount (which we call A_{init}) present in cell 1:

$$A_i(0) = \begin{Bmatrix} A_{\text{init}} & \text{for } i = 1 \\ 0 & \text{for } 2 \leq i \leq n+1 \end{Bmatrix}.$$

We ran our initial simulations at $A_{\text{init}} = 1$. However, to find correlations between wave amplitude, we will be varying the initial concentration later on. Similarly, we assume that initially no PIN1 exists, in either polarized or unpolarized form, in any cell:

$$P_i(0) = 0 \text{ for } 1 \leq i \leq n+1,$$
$$P_{i,j}(0) = 0 \text{ for } 1 \leq i, j \leq n+1.$$

3.2.2 Boundary conditions

As stated before, we also have some boundary conditions. Specifically, the equations we use will look a bit different for cells 1, n and the Auxin sink $n+1$.

For cell 1, we simply eliminate any terms that would require a cell 0. Equation (3.1) becomes

$$\begin{aligned}\frac{dA_1(t)}{dt} =& T_{act}\Big(P_{2,1}(t)\frac{A_2(t)}{k_a + A_2(t)} - P_{1,2}(t)\frac{A_1(t)}{k_a + A_1(t)}\Big) \\ &+ T_{diff}L(A_2(t) - A_1(t)).\end{aligned} \tag{3.8}$$

The equation of PIN1, equation (3.2), becomes:

$$\frac{dP_1(t)}{dt} = -\lambda P_1(t) + k_2 P_{1,2}(t) + \alpha A_1(t) - \delta P_1(t). \tag{3.9}$$

We assume that all PIN1 polarizes towards the right. This means that equation (3.7) will not play a role in cell 1, so we say that

$$\frac{dP_{1,0}(t)}{dt} = 0. \tag{3.10}$$

As for (3.6), it will simplify to

$$\frac{dP_{1,2}(t)}{dt} = \lambda P_1(t) - k_2 P_{1,2}(t). \tag{3.11}$$

For cell n, we will assume that $n+1$ cannot transfer Auxin back. As it represents a much larger system (i.e. the rest of the plant), we set $P_{n+1,n} = 0$ and $A_{n+1} = 0$. This means we have to change the equation for Auxin in cell n. The equations governing PIN1 (in any polarization or lack thereof) remain unchanged.

$$\begin{aligned}\frac{dA_n(t)}{dt} =& T_{act}\Big(P_{n-1,n}(t)\frac{A_{n-1}(t)}{k_a + A_{n-1}(t)} - P_{n,n-1}(t)\frac{A_n(t)}{k_a + A_n(t)} \\ &- P_{n,n+1}(t)\frac{A_n(t)}{k_a + A_n(t)}\Big) + T_{diff}L(A_{n-1}(t) - 2A_n(t))\end{aligned} \tag{3.12}$$

As for the Auxin sink, "cell" $n+1$, we do not care about PIN1 in any way, as we set $P_{n+1,n} = 0$, and there is no cell $n+2$. The only relevant equation is (3.1), concerning Auxin. The equation heavily simplifies to

$$\frac{dA_{n+1}(t)}{dt} = T_{act}P_{n,n+1}(t)\frac{A_n(t)}{k_a + A_n(t)}. \tag{3.13}$$

3.3 Analysis of Auxin

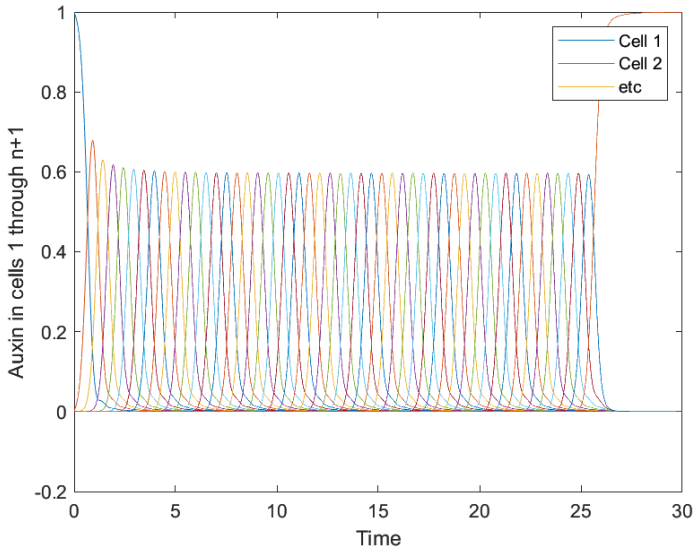

Figure 3.1: Auxin concentrations of cells 1 through n+1 against time. We obtained this graph using equations (3.1), (3.2), (3.6) and (3.7), with $A_{\text{init}} = 1$. Note that the final curve is simply the Auxin sink.

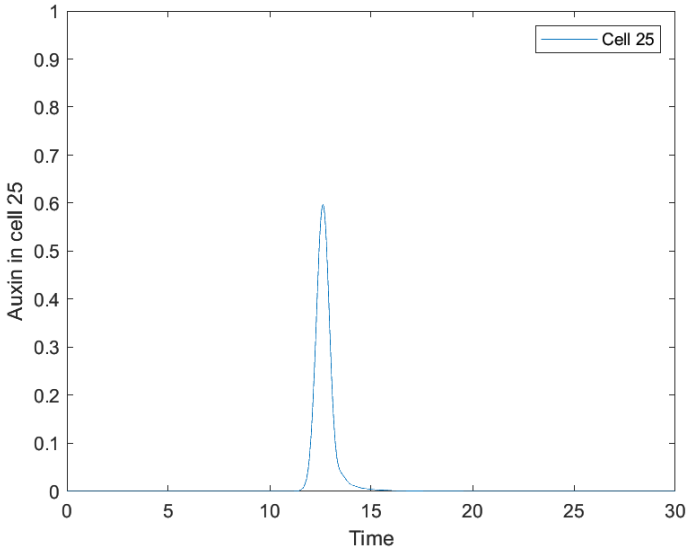

Figure 3.2: Auxin concentration in cell 25, taken from figure 3.1

Running the simulation with the stated equations and initial conditions, yields figure 3.1. As seen, the Auxin moves from left to right in a distinct wave pattern. We will attempt a similar analysis as v.d. Voort [14] by analyzing the waveform. In chapter 4, we will attempt to use the insights obtained in this chapter to find an an analytical solution at leading order.

To analyze this waveform, we will explore the relationship between the amplitude, and the width and the wave speed. To do so, we need to somehow obtain these variables from our data:
To define the wave amplitude (denoted by ϵ), we used MATLAB's 'max' function, to obtain the highest Auxin concentration achieved in individual cells. Then, we averaged over cells $\frac{n+1}{4}$ through $\frac{3(n+1)}{4}$ to get the amplitude.

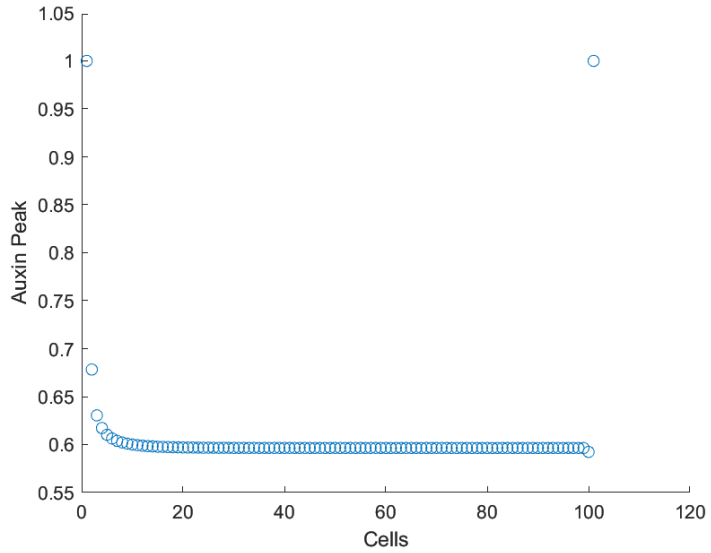

Figure 3.3: The maximum value of Auxin per cell, with $A_{\text{init}} = 1$. The outliers are cells 1 and $n+1$ respectively. The deviating values are due to the boundary conditions.

To model the wave speed (denoted by v), we measured the time between two peaks, and again averaged this value. As this is a time, taking one over this value produces a velocity, which gives us the wave speed.

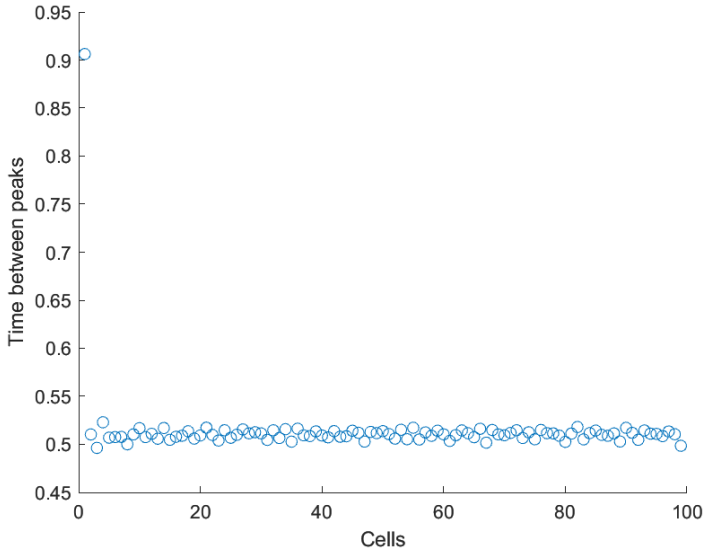

Figure 3.4: The time between peaks at $A_{\text{init}} = 1$; the ith dot represents the time between the peaks of cells i and $i + 1$.

The wave width (denoted by b) is slightly more tricky; first off, we measure the distance from the first time the value of Auxin in a cell reaches 5%, to the second time. As this is really a time, not a distance, we multiply by the wave speed to get the wave width.

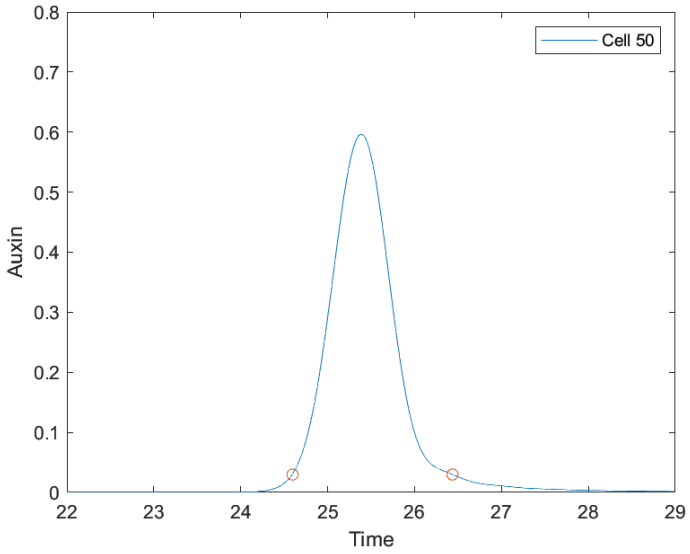

Figure 3.5: The wave sojourn time of cell 50. Marked are the points at which the Auxin concentration is 5% of its maximum. Again, we have $A_{\text{init}} = 1$.

Now that we have established these quantities, we can begin analyzing them. Running the simulation once gives us the wave speed and width for a single amplitude; to find a correlation, we will vary A_{init} in the following sections. This will yield different waves of varying amplitudes, speeds and widths.

3.3.1 Amplitude versus wavespeed

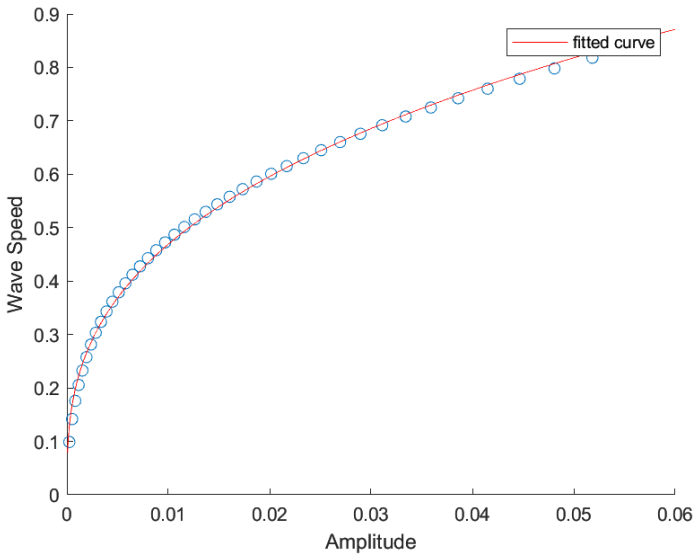

Figure 3.6: The amplitude of the Auxin wave, against its speed.

The first correlation that we examine, is the one between the amplitude of the wave, and the speed. As we can tell, this resembles a root-like relationship. Fitting a curve to the data, we get the following:

$$v \approx 2.3 \cdot \epsilon^{0.35} \tag{3.14}$$

Here the variables v and ϵ represent the wave speed and amplitude respectively.

3.3.2 Amplitude versus wave width

We find a more interesting correlation between the amplitude and the wave width b (or, more usefully, $\frac{1}{b}$);

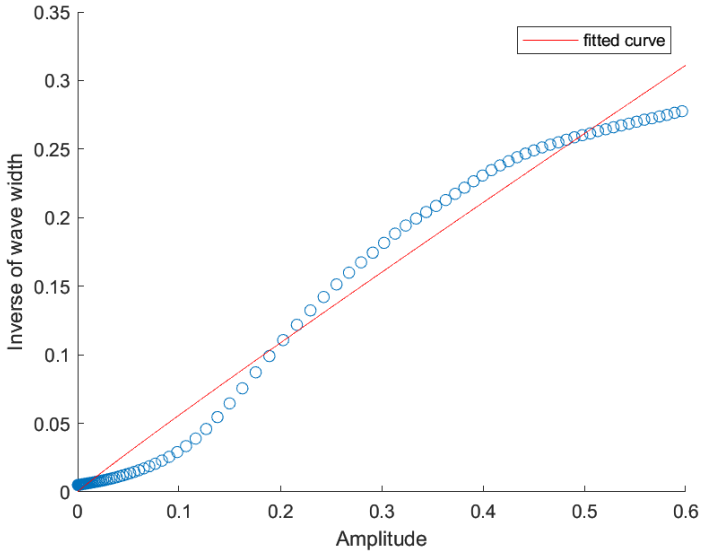

Figure 3.7: The relationship between the wave amplitude, and the inverse of the wave width.

This does not correspond to any simple root-like relationship; rather it appears there are two regimes, separated around $\epsilon \approx 0.2$. We will focus on the smaller regime first. 'Cutting off' larger values of ϵ, we get the plot

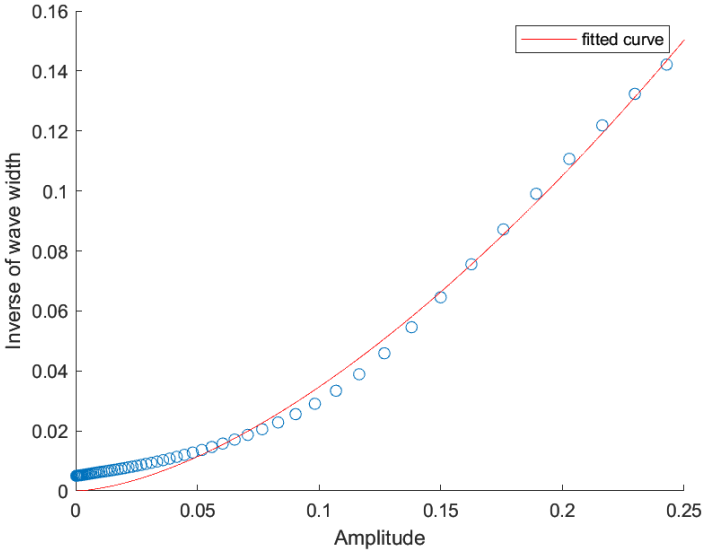

Figure 3.8: The relationship between the wave amplitude, and the inverse of the wave width, for small amplitude.

In the graph above, we fitted the following curve:

$$\frac{1}{b} \approx 1.4 \cdot \epsilon^{1.60} \tag{3.15}$$

3.4 Wave comparison

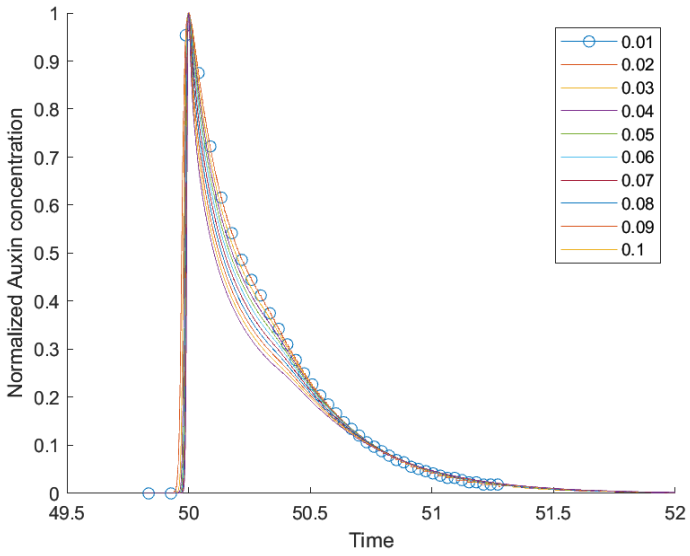

Figure 3.9: Scaled waves for initial Auxin concentrations of 0.01 through 0.1 The wave corresponding to 0.01 is marked with circles.

To qualitatively compare how varying initial Auxin concentrations affect the wave profile, I ran the simulation using initial Auxin concentrations ranging from 0.01 to 0.1. Subsequently, I scaled the concentration in cell 50 both to height 1 and width 1 (both as defined in the previous section). Finally, I also shifted the graphs to have their peaks at the same time; the point at 50 seconds was chosen for convenience, rather than meaning. The results are plotted in figure 3.9.

What we can conclude from this graph, is that as the initial Auxin decreases, the scaled wave becomes more concentrated around the peak, while for smaller Auxin, the tails are slightly wider.

We see that as epsilon becomes smaller, the waves appear to approach the circled blue line. In chapter 4 we will look for a leading order analytical solution; we expect this solution to look like the circled blue line.

3.5 Analysis of RPIN and LPIN

Unlike in the analysis performed by v.d. Voort, we will find in the next section that RPIN and LPIN cannot be analytically solved at first order, from the equations we have. Therefore, we need to take a look at the amplitudes of RPIN, respectively LPIN, and see how they relate to the amplitude of Auxin. We name the amplitude of RPIN η, and the amplitude of LPIN η'. I ran the same simulation as in the previous sections, and the amplitude of RPIN, respectively LPIN, is defined in the same way as the amplitude of Auxin was defined.

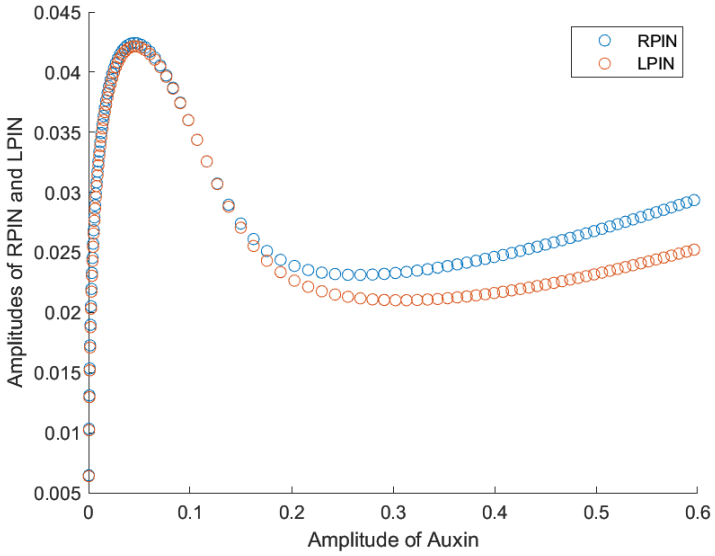

Figure 3.10: ϵ versus η (blue) and η' (orange).

Taking a look at this figure, we see that there is no simple correlation between the 3 variables. However, if we focus on very small ϵ, we see a root-like function.

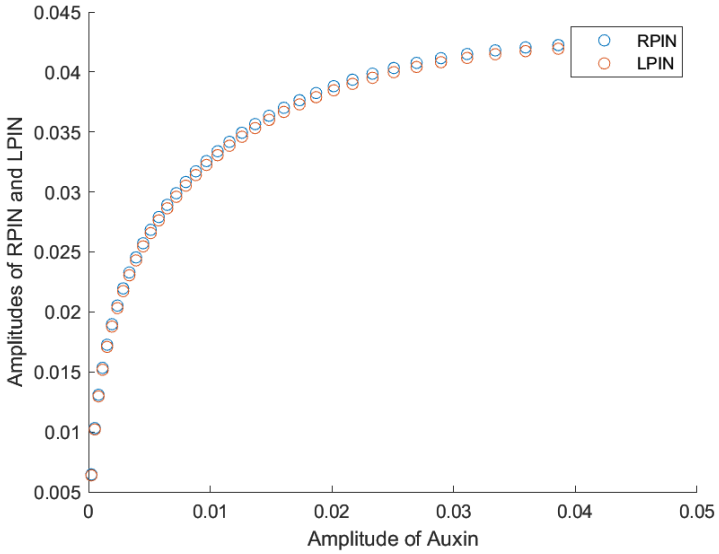

Figure 3.11: ϵ versus η (blue) and η' (orange)

From this graph we can see that for small ϵ, η and η' are almost the same. Performing a fit on the data gives us

$$\eta \approx \eta' \approx 0.1 \cdot \epsilon^{0.25} \tag{3.16}$$

Another interesting property to look at, is the difference between RPIN and LPIN ($P_{i,i+1} - P_{i,i-1}$ to be clear). This quantity will play a role in the Auxin flux in chapter 4. We see that the amplitude of this property is $\eta - \eta'$. Plotting this quantity against the amplitude of Auxin, gives a fascinating result:

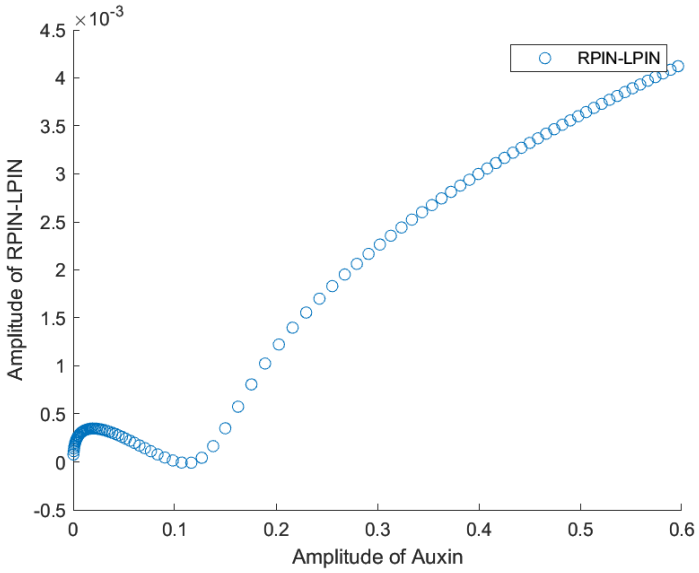

Figure 3.12: ϵ plotted against $\eta - \eta'$

We were unable to find any lower order function to fit to this data. However, if we once again focus on the very small ϵ, we do get a somewhat manageable result:

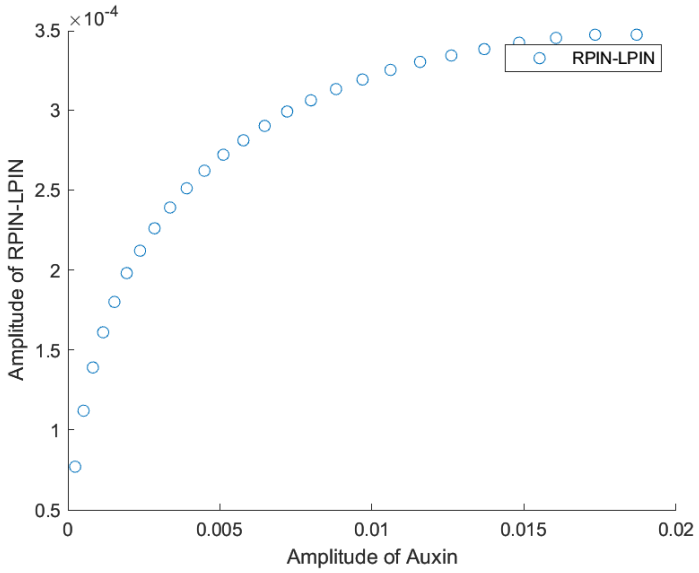

Figure 3.13: ϵ plotted against $\eta - \eta'$, for small ϵ.

We note that once again, we see a root-like relationship here. Performing a fit on the data gives us

$$\eta - \eta' \approx 2.1 \cdot 10^{-3} \cdot \epsilon^{0.41} \tag{3.17}$$

It is important to state here, that while we have restricted ourselves to small ϵ before, we now restrict ourselves much further; where ϵ of the order of 0.1 worked to fit the relationship between the amplitude of Auxin and its width, we now need ϵ of order 0.01.

3.6 In conclusion

Having ran our simulations, we have found the following correlations:

$$v \approx 2.3 \cdot \epsilon^{0.35}$$

$$\frac{1}{b} \approx 1.4 \cdot \epsilon^{1.60}$$

$$\eta \approx 0.1 \cdot \epsilon^{0.25}$$

$$\eta - \eta' \approx 2.1 \cdot 10^{-3} \cdot \epsilon^{0.41}$$

Having found these correlations numerically, we can use them to guide us through our analytical derivation in the next chapter. We will investigate whether this approach will yield the same coefficients, or different ones.

Chapter 4

Leading order analytical solution

In this chapter we will be looking for a leading-order analytical solution. We will start off similar to the analysis by v.d. Voort [14], on the model by Merks [9].

First, we will linearise the equations used in chapter 3, namely equations (3.1), (3.2), (3.6) and (3.7) . Then, we will introduce several wave profiles, which we will expand in terms of ϵ. Using these expansions, we will attempt to solve the linearised equations.

4.1 Linearization

To begin finding an analytical leading order solution, we start with linearizing the equations of the model. The first two equations are easy to deal with: noting that $\frac{1}{k_a}$ is the leading order term for $\frac{1}{k_a+A_i(t)}$, we see that the equation for auxin becomes:

$$\frac{dA_i(t)}{dt} = \frac{T_{act}}{k_a}(P_{i-1,i}(t)A_{i-1}(t) - P_{i,i-1}(t)A_i(t) + P_{i+1,i}(t)A_{i+1}(t) - P_{i,i+1}(t)A_i(t)) + T_{diff}L(A_{i-1}(t) + A_{i+1}(t) - 2A_i(t)) + H.O.T \quad (4.1)$$

We notice that (3.2) is already linearised:

$$\frac{dP_i(t)}{dt} = -\lambda P_i(t) + k_2(P_{i,i+1}(t) + P_{i,i-1}(t)) + \alpha A_i(t) - \delta P_i(t)$$

The third equation is more difficult to process. We remember (3.6) and (3.7) (writing them in a more compact form):

$$\frac{dP_{i,i\pm1}(t)}{dt} = \lambda P_i(t) \cdot H(J^{i\pm}, J^{i\mp}) - k_2 P_{i,i\pm1}(t)$$

With

$$H(J^{i\pm}, J^{i\mp}) = \frac{h_{i\pm}}{h_{i+} + h_{i-}}$$

as defined in (3.5). We note that linearizing this equation, boils down to linearizing $H(J^{i\pm}, J^{i\mp})$. As ϵ will be small, we expect that $J^{i\pm} \approx 0$. We will explicitly linearize $H(J^{i+}, J^{i-})$, the term present in RPIN, noting that the other can be found simply by swapping the arguments. For simplicity we write $x = J^{i+}$ and $y = J^{i-}$. So, to linearize this term around $(0, 0)$, we find:

$$H(0,0) = \frac{1}{2} \tag{4.2}$$

Next up, we calculate some derivatives. From equation (3.4) we find the following:

$$\frac{\partial h_{i+}}{\partial x} = \frac{\frac{h}{\lambda} e^{-h(\frac{x}{\lambda} - \theta)}}{(1 + e^{-h(\frac{x}{\lambda} - \theta)})^2} \tag{4.3}$$

$$\frac{\partial h_{i-}}{\partial y} = \frac{\frac{h}{\lambda} e^{-h(\frac{y}{\lambda} - \theta)}}{(1 + e^{-h(\frac{y}{\lambda} - \theta)})^2} \tag{4.4}$$

$$\frac{\partial h_{i-}}{\partial x} = \frac{\partial h_{i+}}{\partial y} = 0 \tag{4.5}$$

In the numerical analysis we used $\theta = 0$, so we will assume the same here. This leads us to:

$$\frac{\partial H}{\partial x} = \frac{(h_{i+} + h_{i-})\frac{\partial h_{i+}}{\partial x} - h_{i+}(\frac{\partial (h_{i+} + h_{i-})}{\partial x})}{(h_{i+} + h_{i-})^2} = \frac{h_{i-}\frac{\partial h_{i+}}{\partial x}}{(h_{i+} + h_{i-})^2} \tag{4.6}$$

Ergo, using equations (3.4) and (4.3) we find that

$$\frac{\partial H}{\partial x}(0,0) = \frac{h}{8\lambda}. \tag{4.7}$$

Similarly, differentiating with respect to the other argument gives us

$$\frac{\partial H}{\partial y} = \frac{(h_{i+} + h_{i-})\frac{\partial h_{i+}}{\partial y} - h_{i+}(\frac{\partial (h_{i+} + h_{i-})}{\partial y})}{(h_{i+} + h_{i-})^2} = \frac{-h_{i+}\frac{\partial h_{i-}}{\partial y}}{(h_{i+} + h_{i-})^2}. \tag{4.8}$$

Ergo, from equations (3.4) and (4.4) it follows that

$$\frac{\partial H}{\partial y}(0,0) = -\frac{h}{8\lambda}. \tag{4.9}$$

Now, we can use equations (4.2), (4.6) and (4.9) to create a Taylor polynomial. We find:

$$H(x,y) = \frac{1}{2} + \frac{h}{8\lambda}(x - y) + H.O.T. \tag{4.10}$$

As stated before, the linearization is analogous if the arguments were swapped. In fact, we will find that

$$H(y,x) = \frac{1}{2} - \frac{h}{8\lambda}(x-y) + H.O.T. \tag{4.11}$$

Inserting the definitions of x, y, and in turn of $J_{i,\pm}$, we find the leading-order expression.

$$H(J^{i\pm}, J^{i\mp}) = \frac{1}{2} \pm \frac{1}{8}\frac{h\sigma_a}{\lambda}(A_iP_{i,i+1} - A_{i+1}P_{i+1,i} - A_iP_{i,i-1} + A_{i-1}P_{i-1,i}) + H.O.T. \tag{4.12}$$

Inserting this into the equations for polarized PIN gives us

$$\begin{aligned}\frac{dP_{i,i\pm1}}{dt} =& \frac{\lambda P_i}{2} \pm \frac{P_i}{8}h\sigma_a(A_iP_{i,i+1} - A_{i+1}P_{i+1,i} - A_iP_{i,i-1} + A_{i-1}P_{i-1,i}) \\ &- k_2P_{i,i\pm1} + H.O.T.\end{aligned} \tag{4.13}$$

We note that this equation isn't really linearized, as there is an additional factor of P_i. However, it is easy to see that at the lowest order, the equations for RPIN and LPIN are identical, likely leading to a purely diffusive solution.

4.1.1 Final assumptions

We make some additional assumptions to simplify our system:

$$k_a = 1,$$

$$k_2 = \delta = 0.$$

The equations become:

$$\begin{aligned}\frac{dA_i(t)}{dt} =& T_{act}\Big(P_{i-1,i}(t)A_{i-1}(t) - P_{i,i-1}(t)A_i(t) + P_{i+1,i}(t)A_{i+1}(t) \\ &- P_{i,i+1}(t)A_i(t)\Big) + T_{diff}L(A_{i-1}(t) + A_{i+1}(t) - 2A_i(t)),\end{aligned} \tag{4.14}$$

$$\frac{dP_i(t)}{dt} = -\lambda P_i(t) + \alpha A_i(t), \tag{4.15}$$

$$\begin{aligned}\frac{dP_{i,i\pm1}(t)}{dt} =& \frac{\lambda P_i(t)}{2} \pm \frac{P_i(t)}{8}h\sigma_a\Big(A_i(t)P_{i,i+1}(t) - A_{i+1}(t)P_{i+1,i}(t) \\ &- A_i(t)P_{i,i-1}(t) + A_{i-1}(t)P_{i-1,i}(t)\Big).\end{aligned} \tag{4.16}$$

4.2 Wave Ansatz

Before we can start to solve the equation for Auxin, we need to establish what our wave looks like. We take our travelling wave solution to be of the form

$$A_i(t) = \epsilon\phi(\frac{1}{b}(i - vt)) \tag{4.17}$$

Here ϵ is the amplitude of the wave, ϕ is a normalized wave function, b is the wave width, and v is the wave speed, matching the symbols used in the previous section. t represents time, and i marks which cell. As seen in Chapter 3, for small ϵ there exist root-like relationships between the amplitude and both the inverse of the width ($\frac{1}{b}$) and the speed v. Thus, from now on, we will write

$$A_i(t) = \epsilon\phi(\epsilon^\beta(i - c\epsilon^\gamma t)) \tag{4.18}$$

Unlike van der Voort, we will find ourselves unable to analytically solve for $P_{i,i\pm1}$. After extensive unsuccessful attempts to solve these equations, we concluded that more wave-profiles needed to be established. As it turns out, simply creating wave profiles for $P_{i,i\pm1}$ will not lead to useful results. Therefore, we will define two more quantities: the sum of $P_{i,i+1}$ and $P_{i,i-1}$, and the difference thereof;

$$P_{i,+}(t) = P_{i,i+1}(t) + P_{i,i-1}(t), \tag{4.19}$$

$$P_{i,-}(t) = P_{i,i+1}(t) - P_{i,i-1}(t). \tag{4.20}$$

When creating a wave profile for these quantities, an important observation is that everything within the argument of the wavefunction must be the same as within the argument of the wavefunction for Auxin. Any differences encountered will be contained within the wave function itself and the amplitude. Therefore, our new wavefunctions must be of the form:

$$P_{i,+}(t) = \epsilon^\delta\rho_+(\epsilon^\beta(i - c\epsilon^\gamma t)), \tag{4.21}$$

$$P_{i,-}(t) = \epsilon^\zeta\rho_-(\epsilon^\beta(i - c\epsilon^\gamma t)). \tag{4.22}$$

As far as the sum is concerned, we found that it offered little analytical insight. Thus, we only use it to rewrite the equations. The difference on the other hand, is far more interesting.

4.3 Solving for $P_i(t)$

We deal with the easiest equation (and in fact the only we can solve straight away) first. We will solve this equation using the integrating factor method. First, we rewrite:

$$\frac{dP_i(t)}{dt} + \lambda P_i(t) = \alpha A_i(t).$$

We need to find a $\mu(t)$ such that

$$\frac{d\mu(t)}{dt} = \lambda\mu(t).$$

We see that the following suffices:

$$\mu(t) = e^{\int \lambda dt} = e^{\lambda t + c_1}.$$

We multiply the first equation with μ:

$$\mu\frac{dP_i(t)}{dt} + \lambda\mu P_i(t) = \mu\frac{dP_i(t)}{dt} + \frac{d\mu(t)}{dt}P_i(t) = \frac{d(\mu(t)P_i(t))}{dt} = \mu(t)\alpha A_i(t).$$

The first equality follows from the definition of μ. The second equality follows from the chain rule. Solving this gives us:

$$P_i(t) = \frac{1}{\mu(t)}\int_{-\infty}^{t}\mu(s)\alpha A_i(s)ds = e^{-\lambda t}\int_{-\infty}^{t}e^{\lambda s}\alpha A_i(s)ds. \tag{4.23}$$

We notice that the constant c_1 disappears. Lastly, we note that the constant arising from the integration has to be 0, as otherwise $P_i(0) \neq 0$. Now, we can use the profiles defined in the previous section:

$$P_i(t) = e^{-\lambda t}\int_{-\infty}^{t}e^{\lambda s}\alpha\epsilon\phi(\epsilon^{\beta}(i - c\epsilon^{\gamma}s))ds.$$

To evaluate this, we will use integration by parts:

$$\begin{aligned}
P_i(t) &= \alpha\epsilon e^{-\lambda t}\cdot\int_{-\infty}^{t}e^{\lambda s}\phi(\epsilon^{\beta}(i - c\epsilon^{\gamma}s))ds \\
&= \alpha\epsilon e^{-\lambda t}\cdot([\frac{1}{\lambda}e^{\lambda s}\cdot\phi(\epsilon^{\beta}(i - c\epsilon^{\gamma}s))]_{-\infty}^{t} - \int_{-\infty}^{t}\frac{1}{\lambda}e^{\lambda s}\cdot c\epsilon^{\beta+\gamma}\phi'(\epsilon^{\beta}(i - c\epsilon^{\gamma}s))ds) \\
&= \frac{\alpha}{\lambda}\cdot\epsilon\phi(\epsilon^{\beta}(i - c\epsilon^{\gamma}t)) - \alpha\epsilon e^{-\lambda t}\cdot\int_{-\infty}^{t}\frac{1}{\lambda}e^{\lambda s}\cdot c\epsilon^{\beta+\gamma}\phi'(\epsilon^{\beta}(i - c\epsilon^{\gamma}s))ds.
\end{aligned}$$

We see that the integral carries additional factors of ϵ, so we consider it a higher order term. Restricting ourselves to the first term, the equation simplifies:

$$P_i(t) = \frac{\alpha}{\lambda}\cdot\epsilon\phi(\epsilon^{\beta}(i - c\epsilon^{\gamma}t)) = \frac{\alpha}{\lambda}\cdot A_i(t). \tag{4.24}$$

This means that $P_i(t)$ is of the same order as $A_i(t)$. This may qualitatively be understood by considering very small ϵ: in this regime $\frac{dP_i(t)}{dt}$ is close to zero, as the amplitude of the wave profile is very small and the profile is very wide. Substituting $\frac{dP_i(t)}{dt} = 0$ in equation (4.15), we find the same relationship.

4.4 Solving for $A_i(t)$

Now that we have established these wave profiles, we can solve (4.14).

4.4.1 Left hand side

We start our evaluation with the left-hand side:

$$\text{LHS} = \frac{dA_i(t)}{dt}. \tag{4.25}$$

We will do so by inserting the wave ansatz, (4.18). Doing so, we find:

$$\text{LHS} = \frac{d}{dt}\epsilon\phi(\epsilon^\beta(i - c\epsilon^\gamma t)) = -c\epsilon^{1+\beta+\gamma} \cdot \phi'(\epsilon^\beta(i - c\epsilon^\gamma t)). \tag{4.26}$$

We note that this is of order $\epsilon^{1+\beta+\gamma}$.

4.4.2 Right hand side

We take a look at the right-hand side of equation (4.14):

$$\begin{aligned}\text{RHS} =& T_{act}(P_{i-1,i}(t)A_{i-1}(t) - P_{i,i-1}(t)A_i(t) + P_{i+1,i}(t)A_{i+1}(t) - P_{i,i+1}(t)A_i(t)) \\ &+ T_{diff}L(A_{i-1}(t) + A_{i+1}(t) - 2A_i(t)).\end{aligned} \tag{4.27}$$

We split our evaluation into two parts.

Passive transport

We first consider the passive transport term. Our analysis is analogous to that performed by van der Voort [14]:

First, we perform a taylor expansion of $A_{i+1}(t)$, by expanding ϕ around $\epsilon^\beta(i - c\epsilon^\gamma t)$ (note that this is not an expansion in terms of t, but the entire argument of ϕ!). Noting that $\epsilon^\beta(i + 1 - c\epsilon^\gamma t) - \epsilon^\beta(i - c\epsilon^\gamma t) = \epsilon^\beta$:

$$A_{i+1}(t) = \epsilon\phi(\epsilon^\beta(i-c\epsilon^\gamma t))+\epsilon^{1+\beta}\phi'(\epsilon^\beta(i-c\epsilon^\gamma t))+\frac{\epsilon^{2\beta+1}}{2}\phi''(\epsilon^\beta(i-c\epsilon^\gamma t))+\mathcal{O}(\epsilon^{3\beta+1}). \tag{4.28}$$

A similar expansion of $A_{i-1}(t)$ yields:

$$A_{i-1}(t) = \epsilon\phi(\epsilon^\beta(i-c\epsilon^\gamma t))-\epsilon^{1+\beta}\phi'(\epsilon^\beta(i-c\epsilon^\gamma t))+\frac{\epsilon^{2\beta+1}}{2}\phi''(\epsilon^\beta(i-c\epsilon^\gamma t))+\mathcal{O}(\epsilon^{3\beta+1}). \tag{4.29}$$

Considering the sum $A_{i+1}(t) + A_{i-1}(t) - 2A_i(t)$, we note that a lot of terms disappear:

$$A_{i+1}(t) + A_{i-1}(t) - 2A_i(t) = \epsilon^{2\beta+1}\phi''(\epsilon^\beta(i - c\epsilon^\gamma t)) + \mathcal{O}(\epsilon^{3\beta+1}). \tag{4.30}$$

Ultimately, the passive transport term becomes:

$$T_{diff}L(A_{i-1}(t)+A_{i+1}(t)-2A_i(t)) = T_{diff}L\cdot(\epsilon^{2\beta+1}\phi''(\epsilon^\beta(i-c\epsilon^\gamma t))+\mathcal{O}(\epsilon^{3\beta+1})). \tag{4.31}$$

We see that the leading order is $\epsilon^{1+2\beta}$.

Active transport

Up next is the active transport term:

$$\text{ACTIVE} = T_{act}(P_{i-1,i}(t)A_{i-1}(t)-P_{i,i-1}(t)A_i(t)+P_{i+1,i}(t)A_{i+1}(t)-P_{i,i+1}(t)A_i(t)). \tag{4.32}$$

Before we can deal with this, we have to perform the change of variables introduced in section 4.2. We can invert equations (4.19) and (4.20) to give us

$$P_{i,i+1}(t) = \frac{1}{2}(P_{i,+}(t) + P_{i,-}(t)) \tag{4.33}$$

and

$$P_{i,i-1}(t) = \frac{1}{2}(P_{i,+}(t) - P_{i,-}(t)). \tag{4.34}$$

We can then rewrite our equation:

$$\begin{aligned}\text{ACTIVE} =& T_{act}\Big(\frac{1}{2}(P_{i-1,+}(t) + P_{i-1,-}(t))A_{i-1}(t) \\ &+ \frac{1}{2}(P_{i+1,+}(t) - P_{i+1,-}(t))A_{i+1}(t) - P_{i,+}(t)A_i(t)\Big).\end{aligned} \tag{4.35}$$

Similar to the Taylor expansions performed on A_{i-1} earlier, we will expand $P_{i-1,+}$, $P_{i-1,-}$, $P_{i+1,+}$ and $P_{i+1,-}$ in terms of $P_{i,+}$ and $P_{i,-}$ respectively. Rembembering definitions (4.21) and (4.22), this leads us to:

$$\begin{aligned}P_{i-1,+}(t) =& \epsilon^{\delta}\rho_+(\epsilon^{\beta}(i - c\epsilon^{\gamma}t)) - \epsilon^{\beta}\cdot\epsilon^{\delta}\rho'_+(\epsilon^{\beta}(i - c\epsilon^{\gamma}t)) \\ &+ \frac{\epsilon^{2\beta}}{2}\cdot\epsilon^{\delta}\rho''_+(\epsilon^{\beta}(i - c\epsilon^{\gamma}t)) + \mathcal{O}(\epsilon^{3\beta+\delta}),\end{aligned} \tag{4.36}$$

$$\begin{aligned}P_{i+1,+}(t) =& \epsilon^{\delta}\rho_+(\epsilon^{\beta}(i - c\epsilon^{\gamma}t)) + \epsilon^{\beta}\cdot\epsilon^{\delta}\rho'_+(\epsilon^{\beta}(i - c\epsilon^{\gamma}t)) \\ &+ \frac{\epsilon^{2\beta}}{2}\cdot\epsilon^{\delta}\rho''_+(\epsilon^{\beta}(i - c\epsilon^{\gamma}t)) + \mathcal{O}(\epsilon^{3\beta+\delta}).\end{aligned} \tag{4.37}$$

And analogously:

$$\begin{aligned}P_{i-1,-}(t) =& \epsilon^{\zeta}\rho_-(\epsilon^{\beta}(i - c\epsilon^{\gamma}t)) - \epsilon^{\beta}\cdot\epsilon^{\zeta}\rho'_-(\epsilon^{\beta}(i - c\epsilon^{\gamma}t)) \\ &+ \frac{\epsilon^{2\beta}}{2}\cdot\epsilon^{\zeta}\rho''_-(\epsilon^{\beta}(i - c\epsilon^{\gamma}t)) + \mathcal{O}(\epsilon^{3\beta+\zeta}),\end{aligned} \tag{4.38}$$

$$\begin{aligned}P_{i+1,-}(t) =& \epsilon^{\zeta}\rho_-(\epsilon^{\beta}(i - c\epsilon^{\gamma}t)) + \epsilon^{\beta}\cdot\epsilon^{\zeta}\rho'_-(\epsilon^{\beta}(i - c\epsilon^{\gamma}t)) \\ &+ \frac{\epsilon^{2\beta}}{2}\cdot\epsilon^{\zeta}\rho''_-(\epsilon^{\beta}(i - c\epsilon^{\gamma}t)) + \mathcal{O}(\epsilon^{3\beta+\zeta}).\end{aligned} \tag{4.39}$$

Finally, we may start to fill in the equation we have. For the sake of brevity, we

will write the argument as $\chi(i,t) = \epsilon^{\beta}(i - c\epsilon^{\gamma}t)$. Starting with the active part:

$$\begin{aligned}
\text{ACTIVE} = T_{act}(&\frac{1}{2}(\epsilon^{\delta}\rho_{+}(\chi(i,t)) - \epsilon^{\beta}\cdot\epsilon^{\delta}\rho'_{+}(\chi(i,t)) + \frac{\epsilon^{2\beta}}{2}\cdot\epsilon^{\delta}\rho''_{+}(\chi(i,t)) + \mathcal{O}(\epsilon^{3\beta+\delta}) \\
&+ \epsilon^{\zeta}\rho_{-}(\chi(i,t)) - \epsilon^{\beta}\cdot\epsilon^{\zeta}\rho'_{-}(\chi(i,t)) + \frac{\epsilon^{2\beta}}{2}\cdot\epsilon^{\zeta}\rho''_{-}(\chi(i,t)) + \mathcal{O}(\epsilon^{3\beta+\zeta})) \\
&\cdot(\epsilon\phi(\chi(i,t)) - \epsilon^{1+\beta}\phi'(\chi(i,t)) + \frac{\epsilon^{2\beta+1}}{2}\phi''(\chi(i,t)) + \mathcal{O}(\epsilon^{3\beta+1})) \\
&+ \frac{1}{2}((\epsilon^{\delta}\rho_{+}(\chi(i,t)) + \epsilon^{\beta}\cdot\epsilon^{\delta}\rho'_{+}(\chi(i,t)) + \frac{\epsilon^{2\beta}}{2}\cdot\epsilon^{\delta}\rho''_{+}(\chi(i,t)) + \mathcal{O}(\epsilon^{3\beta+\delta})) \\
&- (\epsilon^{\zeta}\rho_{-}(\chi(i,t)) + \epsilon^{\beta}\cdot\epsilon^{\zeta}\rho'_{-}(\chi(i,t)) + \frac{\epsilon^{2\beta}}{2}\cdot\epsilon^{\zeta}\rho''_{-}(\chi(i,t)) + \mathcal{O}(\epsilon^{3\beta+\zeta})) \\
&\cdot(\epsilon\phi(\chi(i,t)) + \epsilon^{1+\beta}\phi'(\chi(i,t)) + \frac{\epsilon^{2\beta+1}}{2}\phi''(\chi(i,t)) + \mathcal{O}(\epsilon^{3\beta+1}))) \\
&- (\epsilon^{\delta}\rho_{+}(\chi(i,t)))\cdot\epsilon\phi(\chi(i,t)))
\end{aligned}$$

This is a frankly monstrous expression. Fortunately, we can simplify it somewhat. Given that the diffusive term is of order $\epsilon^{1+2\beta}$, we will drop any higher order terms. We work out the brackets, to give us

$$\begin{aligned}
\text{ACTIVE} = T_{act}(&\frac{1}{2}(\epsilon^{1+\delta}\rho_{+}(\chi(i,t))\phi(\chi(i,t)) - \epsilon^{1+\beta+\delta}\rho_{+}(\chi(i,t))\phi'(\chi(i,t)) \\
&+ \frac{\epsilon^{1+2\beta+\delta}}{2}\rho_{+}(\chi(i,t))\phi''(\chi(i,t)) - \epsilon^{1+\beta+\delta}\rho'_{+}(\chi(i,t))\phi(\chi(i,t)) \\
&+ \epsilon^{1+2\beta+\delta}\rho'_{+}(\chi(i,t))\phi'(\chi(i,t)) + \frac{\epsilon^{1+2\beta+\delta}}{2}\rho''_{+}(\chi(i,t))\phi(\chi(i,t)) \\
&+ \epsilon^{1+\zeta}\rho_{-}(\chi(i,t))\phi(\chi(i,t)) - \epsilon^{1+\beta+\zeta}\rho_{-}(\chi(i,t))\phi'(\chi(i,t)) \\
&+ \frac{\epsilon^{1+2\beta+\zeta}}{2}\rho_{-}(\chi(i,t))\phi''(\chi(i,t)) - \epsilon^{1+\beta+\zeta}\rho'_{-}(\chi(i,t))\phi(\chi(i,t)) \\
&+ \epsilon^{1+2\beta+\zeta}\rho'_{-}(\chi(i,t))\phi'(\chi(i,t)) + \frac{\epsilon^{1+2\beta+\zeta}}{2}\rho''_{-}(\chi(i,t))\phi(\chi(i,t))) \\
&+ \frac{1}{2}(\epsilon^{1+\delta}\rho_{+}(\chi(i,t))\phi(\chi(i,t)) + \epsilon^{1+\beta+\delta}\rho_{+}(\chi(i,t))\phi'(\chi(i,t)) \\
&+ \frac{\epsilon^{1+2\beta+\delta}}{2}\rho_{+}(\chi(i,t))\phi''(\chi(i,t)) + \epsilon^{1+\beta+\delta}\rho'_{+}(\chi(i,t))\phi(\chi(i,t)) \\
&+ \epsilon^{1+2\beta+\delta}\rho'_{+}(\chi(i,t))\phi'(\chi(i,t)) + \frac{\epsilon^{1+2\beta+\delta}}{2}\rho''_{+}(\chi(i,t))\phi(\chi(i,t)) \\
&- \epsilon^{1+\zeta}\rho_{-}(\chi(i,t))\phi(\chi(i,t)) - \epsilon^{1+\beta+\zeta}\rho_{-}(\chi(i,t))\phi'(\chi(i,t)) \\
&- \frac{\epsilon^{1+2\beta+\zeta}}{2}\rho_{-}(\chi(i,t))\phi''(\chi(i,t)) - \epsilon^{1+\beta+\zeta}\rho'_{-}(\chi(i,t))\phi(\chi(i,t)) \\
&- \epsilon^{1+2\beta+\zeta}\rho'_{-}(\chi(i,t))\phi'(\chi(i,t)) - \frac{\epsilon^{1+2\beta+\zeta}}{2}\rho''_{-}(\chi(i,t))\phi(\chi(i,t))) \\
&- \epsilon^{1+\delta}\rho_{+}(\chi(i,t))\phi(\chi(i,t)) + \mathcal{O}(\epsilon^{1+3\beta}))
\end{aligned}$$

This isn't really any simpler. However, if we start matching terms of the same order, we will notice that a great deal of terms cancel out or simplify.

$$\begin{aligned}\text{ACTIVE} =& T_{act}\Big(\frac{1}{2}(\epsilon^{1+2\beta+\delta}(\rho_+(\chi(i,t))\phi''(\chi(i,t)) \\ &+ 2\rho'_+(\chi(i,t))\phi'(\chi(i,t)) + \rho''_+(\chi(i,t))\phi(\chi(i,t))))\Big) \\ &- T_{act}\Big(\epsilon^{1+\beta+\zeta}(\rho_-(\chi(i,t))\phi'(\chi(i,t)) + \rho'_-(\chi(i,t))\phi(\chi(i,t)))\Big) + \mathcal{O}(\epsilon^{1+3\beta})\end{aligned}$$

Putting this together with the passive transport part of the equation, we find:

$$\text{RHS} = \text{ACTIVE} + T_{diff}L\cdot(\epsilon^{2\beta+1}\phi''(\chi(i,t))) + \mathcal{O}(\epsilon^{3\beta+1})). \tag{4.40}$$

4.4.3 The full equation of Auxin

Then, the completed equation becomes:

$$-c\epsilon^{1+\beta+\gamma}\cdot\phi'(\chi(i,t)) = \text{ACTIVE} + T_{diff}L\cdot(\epsilon^{2\beta+1}\phi''(\chi(i,t)) + \mathcal{O}(\epsilon^{3\beta+1})). \tag{4.41}$$

Now, we will look for the leading order terms. Using equations (4.26) and (4.40), we have:

$$\begin{aligned}-c\epsilon^{1+\beta+\gamma}\cdot\phi'(\chi(i,t)) =& T_{act}\Big(\frac{1}{2}(\epsilon^{1+2\beta+\delta}(\rho_+(\chi(i,t))\phi''(\chi(i,t)) \\ &+ 2\rho'_+(\chi(i,t))\phi'(\chi(i,t)) + \rho''_+(\chi(i,t))\phi(\chi(i,t))))\Big) \\ &- T_{act}\Big(\epsilon^{1+\beta+\zeta}(\rho_-(\chi(i,t))\phi'(\chi(i,t)) + \rho'_-(\chi(i,t))\phi(\chi(i,t)))\Big) \\ &+ T_{diff}L\cdot(\epsilon^{2\beta+1}\phi''(\chi(i,t))) + \mathcal{O}(\epsilon^{1+3\beta}).\end{aligned} \tag{4.42}$$

We notice that the first active transport term is a higher order term, so we disregard it. This leaves us with the following equation:

$$-c\epsilon^{1+\beta+\gamma}\cdot\phi' = -T_{act}\cdot\epsilon^{1+\beta+\zeta}(\phi\rho'_- + \phi'\rho_-) + T_{diff}L\cdot(\epsilon^{2\beta+1}\phi''). \tag{4.43}$$

As our experimental observations suggested that $\beta \approx 1.6$, we believe the diffusive term to be higher order as well. Matching the lower order terms gives us

$$\gamma = \zeta. \tag{4.44}$$

We note that in chapter 3 we found $\gamma = 0.3459$ and $\zeta = 0.4089$. While these values do not match, the 95% confidence intervals overlap to a reasonable extent. However, we will now try to deduce an analytical value for these parameters.

4.5 Solving for $P_{i\pm1}(t)$

As we still do not have enough information to determine the exponents, we will perform a similar analysis for $P_{i\pm1}(t)$, using equations (4.16). These were:

$$\frac{dP_{i,i\pm1}(t)}{dt} = \frac{\lambda P_i(t)}{2} \pm \frac{P_i(t)}{8} h\sigma_a (A_i(t)P_{i,i+1}(t) - A_{i+1}(t)P_{i+1,i}(t) - A_i(t)P_{i,i-1}(t) + A_{i-1}(t)P_{i-1,i}(t))$$

4.5.1 Changing variables

For the sake of brevity, we say that

$$\frac{dP_{i,i\pm1}(t)}{dt} = \frac{P_i(t)}{2}(\lambda \pm \frac{1}{4} h\sigma_a F_i(t)) \tag{4.45}$$

with a 'Flux-term':

$$F_i(t) = A_i(t)P_{i,i+1}(t) - A_{i+1}(t)P_{i+1,i}(t) - A_i(t)P_{i,i-1}(t) + A_{i-1}(t)P_{i-1,i}(t). \tag{4.46}$$

We note that this term is strikingly similar to the active transport term in the equation of Auxin, however it differs in two signs. As stated in section 4.3, if we consider the polarized versions PIN1 on their own, we will find that to a leading order they are the same, as the λ-term dominates in the differential equation. In turn, this leads to a solution that is diffusive, rather than active. Again, we will use the difference between RPIN and LPIN, and the sum of these.

First, we will examine the sum. We notice that the differential equation for $P_{i,+}$ is as follows:

$$\frac{dP_{i,+}}{dt} = \frac{dP_{i,i+1}}{dt} + \frac{dP_{i,i-1}}{dt} = \lambda P_i. \tag{4.47}$$

It is easy to see that this is simply twice the leading order of equation (4.45), so no new information is contained in this statement. What is more interesting is the differential equation we see when we consider the difference:

$$\frac{dP_{i,-}}{dt} = \frac{1}{4} P_i(t) h\sigma_a F_i. \tag{4.48}$$

4.5.2 Left-hand side

We start off with the left-hand side of equation (4.48):

$$\text{LHS} = \frac{dP_{i,-}}{dt} \tag{4.49}$$

From equation (4.22) we easily find that

$$\text{LHS} = -c\epsilon^{\beta+\gamma+\zeta}\rho'_-(\epsilon^\beta(i - c\epsilon^\gamma t)). \tag{4.50}$$

4.5.3 Right-hand side

The right-hand side of equation (4.48) is somewhat more complicated:

$$\text{RHS} = \frac{1}{4} P_i(t) h \sigma_a F_i(t). \tag{4.51}$$

For this side, we start our evaluation in $F_i(t)$. Written in terms of the sum and difference, the term looks like

$$F_i = A_i(t)P_{i,-}(t) - \frac{1}{2}\cdot(A_{i+1}(t)(P_{i+1,+}(t) - P_{i+1,-}(t)) - A_{i-1}(t)(P_{i-1,+}(t) + P_{i-1,-}(t))). \tag{4.52}$$

We notice from equation (4.48) that we will deal with additional factors of ϵ, resulting from a factor $P_i(t)$, so we will focus on the lowest order terms. We use the expansions and definitions we used before to find:

$$F_i(t) = 2\epsilon^{1+\zeta}\phi(\chi(i,t))\rho_-(\chi(i,t)). \tag{4.53}$$

Putting this into (4.51), we are left with the following:

$$\text{RHS} = \frac{\alpha h \sigma_a}{2\lambda}\epsilon^{2+\zeta}\phi^2(\chi(i,t))\rho_-(\chi(i,t)). \tag{4.54}$$

4.5.4 The full equation for $P_{i,-}(t)$

We can now finally equate the left-hand-side and right-hand side. Putting equations (4.50) and (4.54) together gives us:

$$-c\epsilon^{\beta+\gamma+\zeta}\rho'_-(\chi(i,t)) = \frac{\alpha h \sigma_a}{2\lambda}\epsilon^{2+\zeta}\phi^2(\chi(i,t))\rho_-(\chi(i,t)). \tag{4.55}$$

If these terms are to be of the same order ϵ, we require that $\beta + \gamma + \zeta = 2 + \zeta$. In other words:

$$\beta + \gamma = 2. \tag{4.56}$$

4.6 In conclusion

Despite my best efforts, I can not yet find an analytical value for β, γ, δ and ζ. However, the relationships we have found between these parameters appear to be supported by numerical analysis; in section 4.3, equation (4.43) gives us

$$\gamma = \zeta.$$

And in the previous section, we concluded from (4.55) that

$$\beta + \gamma = 2.$$

Both of these claims are supported by the values of these parameters we found in chapter 3:

$$\begin{aligned}\beta &\approx 1.6,\\ \gamma &\approx 0.35,\\ \delta &\approx 0.25,\\ \zeta &\approx 0.41.\end{aligned}$$

While the analytical claims do not mach the exact values, they are well within the 95% confidence intervals of the measurements. On a final note, we see that no analytical prediction has been found for δ. To do so, we will have to take into account higher order terms in the expansions and equations. Doing so, however, would take too much time at this point, and thus we move on to the final part of this thesis.

Chapter 5

Wave trains

Having worked our way through both numerical analysis and analytical approximation, we finally arrive at the concept of wave trains. Up until this point, we have assumed a certain initial concentration of Auxin in cell 1. Going forward, we rather assume a constant influx of Auxin throughout the simulation. For both the model by Merks (equations (2.1), (2.4) and (2.5)), as well as the adapted model (equations (3.1), (3.2), (3.6) and (3.7)), I will explore the relationship between wave amplitude and width, and compare these both to the case of fixed initial Auxin, as well as to the other model.

To simulate a constant influx, we made two major changes. First off, we set the initial Auxin concentration to zero in all cells (as opposed to zero in all but one cell). In other words:

$$A_i(0) = \big\{0 \text{ for } 1 \leq i \leq n+1\big\}$$

Since this would make for a boring model on its own, we modified the differential equation for Auxin in cell 1 to have an added constant. The complete code used can be found in appendix A.4:

$$\begin{aligned}\frac{dA_1(t)}{dt} =& T_{act}(P_{2,1}(t)\frac{A_2(t)}{k_a + A_2(t)} - P_{1,2}(t)\frac{A_1(t)}{k_a + A_1(t)}) \\ &+ T_{diff}L(A_2(t) - A_1(t)) + 0.1. \end{aligned} \tag{5.1}$$

We note that equations for Auxin in the other cells (equation (3.1)), as well as the equations for PIN1, RPIN and LPIN (equations (3.2), (3.6) and (3.7)) remain unchanged.

Finally, to properly compare the two models, we have to rephrase the model by Merks in terms of our cell configuration as well (as we did in chapter 3). Noticing that the equation for Auxin is the same as in the model by Allen, this gives us the following equations for PIN1 and polarized PIN1:

$$\begin{aligned}\frac{dP_i(t)}{dt} =& -k_1(\frac{R \cdot A_{i-1}(t)}{k_R + A_{i-1}(t)}\frac{P_i(t)}{k_m + P_i(t)} + \frac{R \cdot A_{i+1}(t)}{k_R + A_{i+1}(t)}\frac{P_i(t)}{k_m + P_i(t)}) \\ &+ k_2(P_{i,i+1}(t) + P_{i,i-1}(t)) + \alpha A_i(t) - \delta P_i(t) \end{aligned} \tag{5.2}$$

$$\frac{dP_{i,i\pm1}(t)}{dt} = k_1 \frac{R \cdot A_{i\pm1}(t)}{k_R + A_{i\pm1}(t)} \frac{P_i(t)}{k_m + P_i(t)} - k_2 P_{i,i\pm1}(t) \tag{5.3}$$

Qualitatively, we find that in both models Auxin builds up in a cell. After reaching a certain concentration, the hormone is sent out through the line of cells. Afterwards, Auxin starts building up again, and the process repeats. In figure 5.2 we see three 'packets' produced in the model by Merks. In figure 5.6, we see many more packets produced by the modified model.

Exploring the varying connections in this new regime, proves to be somewhat more difficult. As it turns out, each 'wave packet' manifests later in the sequence of cells; while an earlier packet may start at cell 10, a later one might only start at cell 20. As such, I have elected to look at a single cell, in multiple packets, to determine the relationship between amplitude and wave width. A drawback of this, is that the wave speed is ill-defined, which means that we will also have to make due with the wave sojourn time, rather than the actual width.

To measure the different peaks, we first chopped up the wave train into separate waves by using the 'islocalmin' function in Matlab.

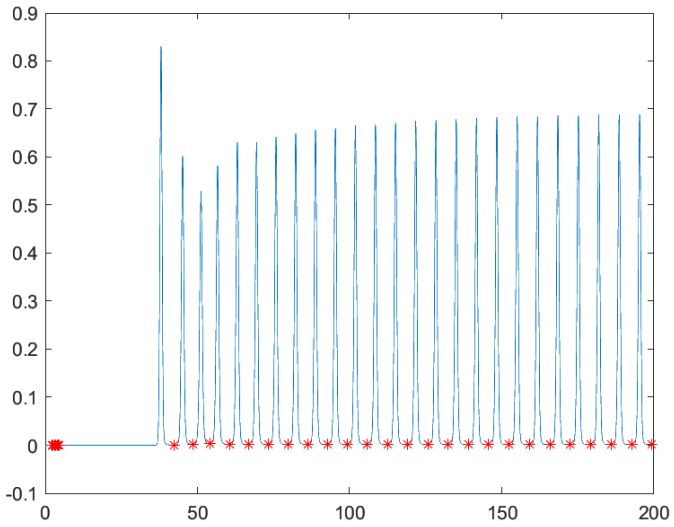

Figure 5.1: Local minima of cell 60 in the modified model

The first few minima (around 0) are meaningless, so we ignore them. Within each of the resulting intervals we measure the peak and wave sojourn time as done in chapter 3: using the max function, and finding the first and last value where the function exceeds 5% of this maximum.

Ultimately, we found rather few data points using only one constant influx. To solve this, I ran the simulation multiple times, at different Auxin influx.

5.1 The model by Merks

An important note to make here is that a modification had to be made to this model: van der Voort [14] originally used a PIN1 decay parameter of 0.0001. While for an initial condition of Auxin this produced a nice traveling wave, for a constant influx, the PIN1 did not decay fast enough to generate a new wave packet. To mitigate this, I raised this parameter to 0.1.
Running the simulation in this altered form gives us the following wave pattern:

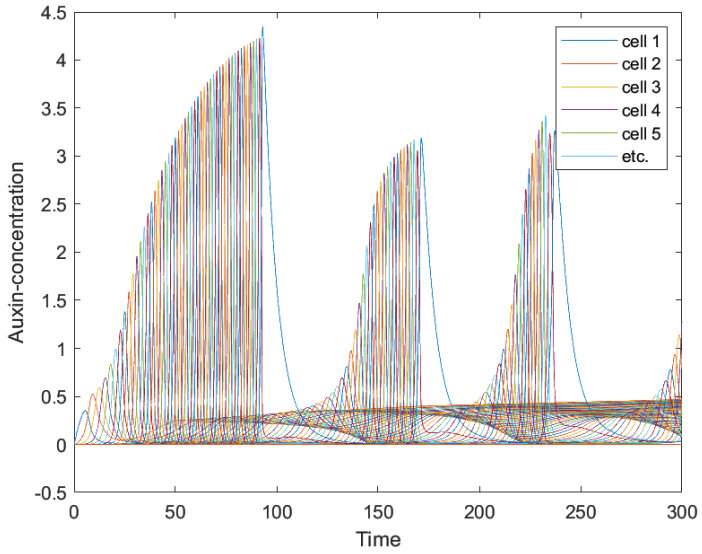

Figure 5.2: Wave Trains in the model by Merks (equations (5.1), (3.1),(5.2), (5.3))

We specifically consider cell 50, as the observed wave profile is pronounced enough to draw conclusions, and it barely suffers from border conditions.

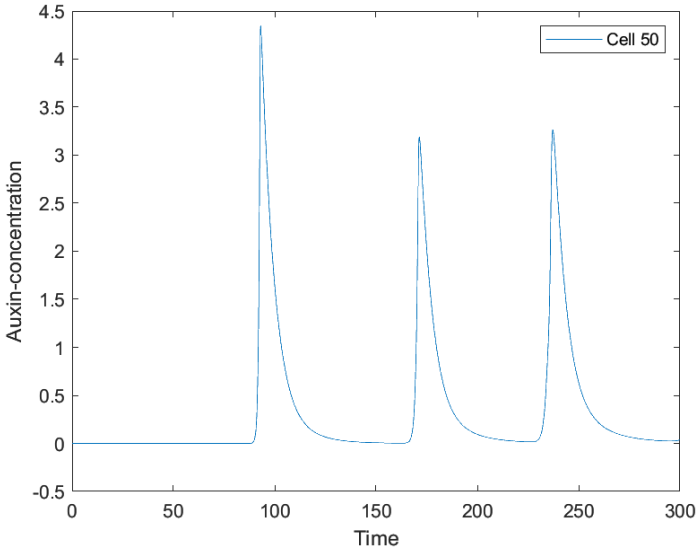

Figure 5.3: Wave Trains in cell 50, in the model by Merks (equations (5.1),(3.1),(5.2), (5.3)).

Now, analogous to chapter 3 we correlate the amplitude and wave sojourn times of these peaks:

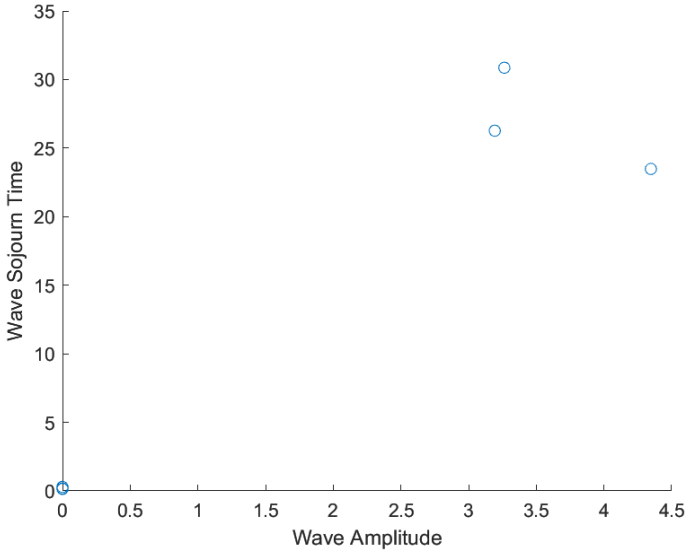

Figure 5.4: Peaks of cell 50 matched against corresponding wave sojourn times, as generated by the model by Merks (equations (3.1), (5.1)-(5.3)).

There are too few data points to draw any reliable conclusion. To resolve this, I ran multiple simulations at differing influxes of Auxin. These attempts to expand the amount of data have been met with errors by Matlab; the equation does not converge fast enough, and my computer runs out of RAM, forcing Matlab to terminate the calculation. I can only conclude that there is no correlation to be seen here, for lack of data.

What we find for a fixed initial amount of Auxin is also quite interesting. Due to PIN1 decay being much higher, we find that in the original model (with fixed initial concentration), Auxin does not produce a traveling wave; much less a reliable correlation between the amplitude and width thereof.

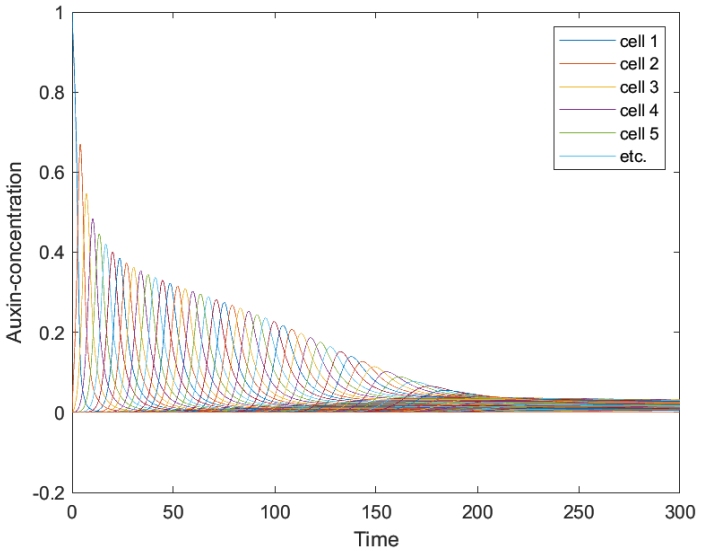

Figure 5.5: Auxin development at fixed initial Auxin, with high PIN1 decay, model by Merks (equations (3.1),(5.2), (5.3))

Again, we can draw no reliable conclusion here, as the transport is quite passive. As stated before, using the parameter used by van der Voort leads to the simulation for the constant influx failing. At this point, we can only conclude that the parameter regimes of the fixed initial Auxin and the constant influx for the model by Merks are simply too different to draw any parallels.

5.2 The Modified model

In the modified model (equations (3.1), (3.2), (3.6), (3.7) and (5.1)) we are met by a very different wave pattern: see figure 5.6

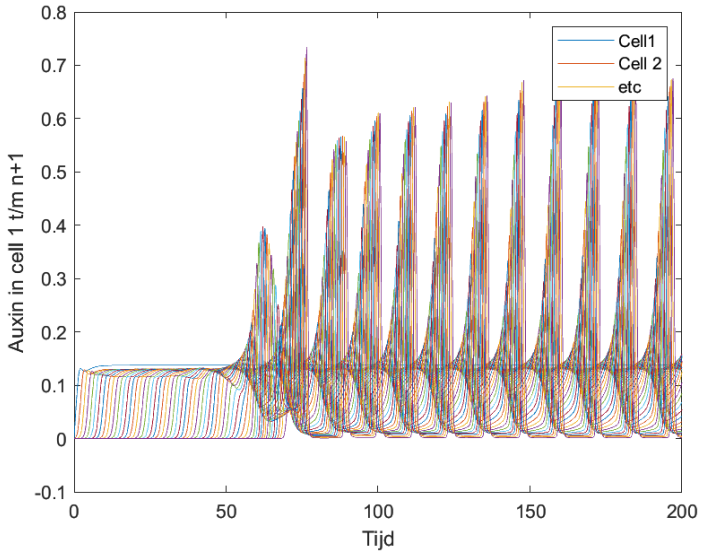

Figure 5.6: Wave trains in cells 1 through 100, generated in modified model (equations (3.1), (3.2), (3.6), (3.7) and (5.1)).

In the modified model, we have a few more cells, so we consider cell 60. We see that we have far more peaks, and therefore more data. We measure the data in the same way as described in the previous section.

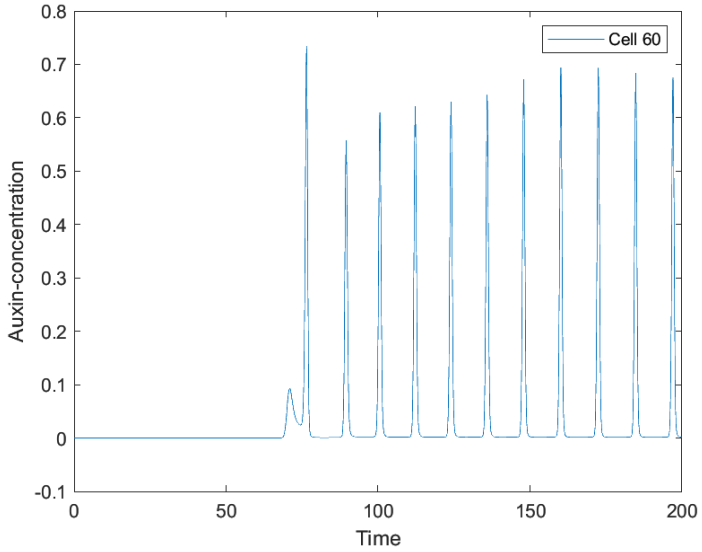

Figure 5.7: Wave train in cell 60, in the modified model (equations (3.1), (3.2), (3.6), (3.7) and (5.1)).

We can now plot the found Auxin peaks against the wave sojourn times. Doing so gives us a far more useful plot than for the model by Merks:

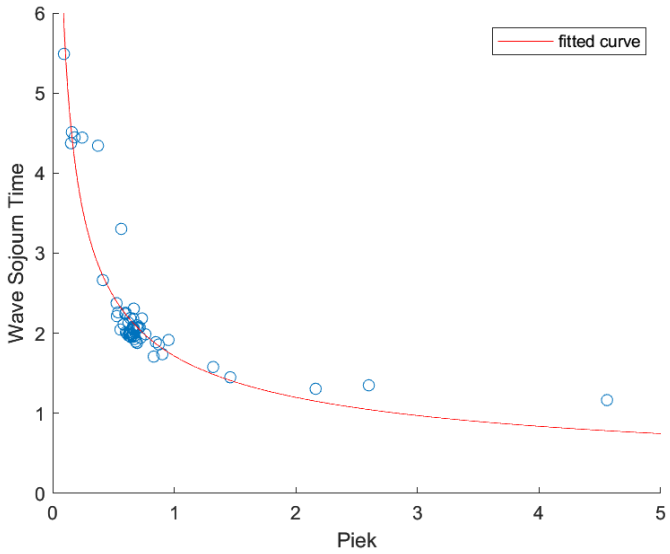

Figure 5.8: Amplitude versus Wave Sojourn Time, as generated by the modified model with a constant Auxin influx (equations (3.1), (3.2), (3.6), (3.7) and (5.1))

In spite of the few datapoints, we see a correlation here. The fitted curve represents the correlation

$$\text{Wave Sojourn Time} = 1.718 \cdot \text{Amplitude}^{-0.5177}. \tag{5.4}$$

Again we compare this to the correlation between amplitude and Wave Sojourn Time in the case of a fixed initial Auxin concentration:

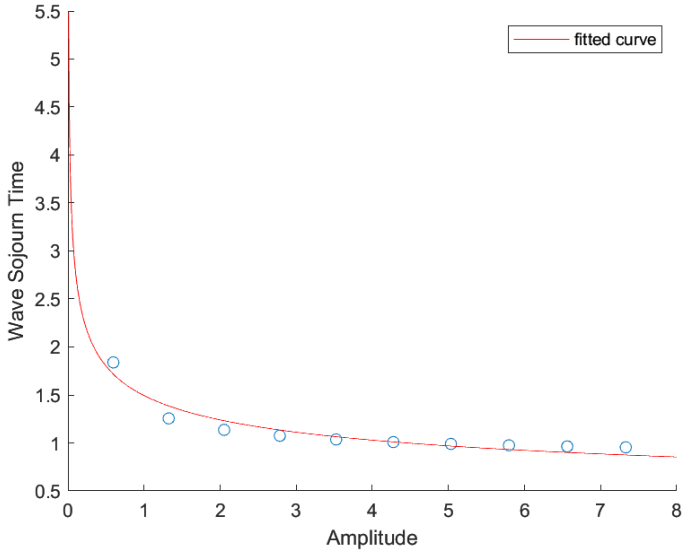

Figure 5.9: Amplitude versus Wave Sojourn Time, as generated by the modified model with fixed initial Auxin (equations (3.1), (3.2), (3.6) and (3.7)). The red line corresponds to the fit in equation (5.5).

This returns a root-like relationship. Having fitted the data, we retrieve

$$\text{Wave Sojourn Time} = 1.527 \cdot \text{Amplitude}^{-0.2865}. \tag{5.5}$$

We note that while they are not identical, the relationships are qualitatively the same, and not too far off each other. We may thus conclude that understanding singular waves will help studying and understanding wave trains. In fact, if we plot the data from figure 5.9 against the fit from figure 5.8, we see a decent match:

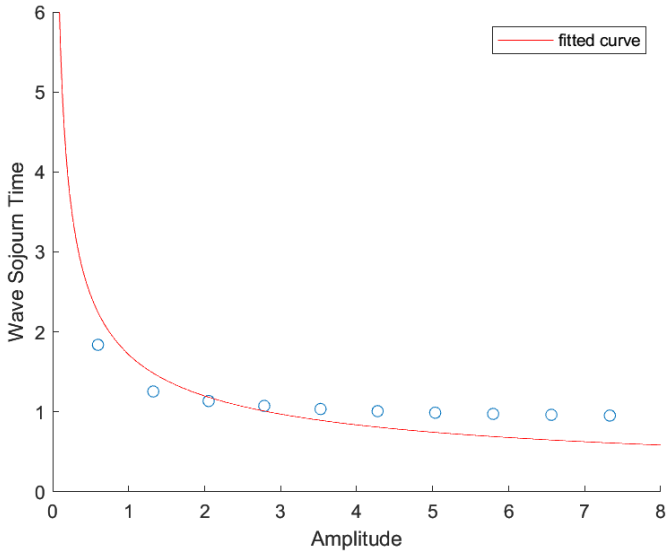

Figure 5.10: Data obtained from a simulation with fixed initial Auxin, set against a fit obtained from a simulation with constant Auxin influx (equations (3.1), (3.2), (3.6), (3.7) and (5.1)). The fitted line is the same as in figure 5.8, corresponding to equation (5.4).

Chapter 6

Discussion

The goal of my thesis was twofold. The first goal was to find a leading order analytical solution that matches the numerically obtained data. On this front, I found that finding such a solution requires including higher order terms; sticking to the lowest order term does not provide analytical values for all parameters involved. As for the second goal, I aimed to prove that in the case of a continuous influx of Auxin into a system, the Auxin would be passed along in wave trains. In chapter 5 I found that this is very much the case: the Auxin is 'stored' for a while and then released, after which the cycle repeats.

I started off by numerical analysis. Doing so, I found that the determined correlations between the wave properties behaved in odd ways for larger amplitudes. To retrieve any useful relation, I had to restrict myself to smaller amplitudes than van der Voort did in his thesis; where an amplitude of order 0.1 [14] sufficed for him, I required an amplitude of order 0.01.

This issue also occurred in the analytical analysis: I found that nonlinear behaviour occurred much earlier than in the original model. While van der Voort was able to describe his wave solution with lower order terms, our model requires the inclusion of higher order terms. However, time constraints required me to abandon these, which might have provided more insight into the properties of the wave. Another problem here was that solving the differential equations for RPIN and LPIN directly created a recursion, which forced the introduction of more wave profiles, with yet more parameters.

Finally, I moved on to the second goal: wave trains. While the original model failed to provide a conclusion on account of the lack of data, the modified model provided us with a fairly strong suggestion that these trains may indeed occur.

I found a few difficulties in using Matlab. Most notably, while examining wave trains in section 5.1, Matlab often failed to run the simulation, when varying the influx of Auxin. In turn, this meant little data could be collected. I also found that running the simulation for fixed Auxin tended to return an error if the chosen parameters did not heavily favour RPIN polarization over LPIN polarization. Some of these issues may be solved (or at the very least diminished) by using a computer with larger amounts of RAM. On a positive note, running

the simulation of the modified model with the parameters I ended up using was much faster than running the original model; therefore, it was possible to run this simulation for longer time spans.

Finally, I can say that much remains to be examined here. As stated, the analytical approximation of the wave in the modified model warrants the introduction of higher order terms. Doing so should lead to a proper analytical solution. Once this particular model has been properly researched, there are several possibilities. The first thing to come to mind, is to fully convert the model into the model used by Allen [3]. Another avenue of potential research is adding a second dimension of cells (or a third, if one is feeling daring). However, while theoretical models are fascinating, it remains equally important to verify their accuracy. It would be interesting to see how the amplitude, speed and wave width of Auxin relate in the real world. As van der Voort put it "...the ball is now in the court of (mathematical) biologists" [14].

Bibliography

[1] Plant morphology. https://en.wikipedia.org/wiki/Plant_morphology.

[2] Reaction diffusion system. https://en.wikipedia.org/wiki/Reaction%E2%80%93diffusion_system.

[3] Henry R. Allen and Mariya Ptashnyk. Mathematical modelling of auxin transport in plant tissues: Flux meets signalling and growth. *Bulletin of Mathematical Biology*, 82(2), 2020.

[4] Tom Bennett, Geneviève Hines, and Ottoline Leyser. Canalization: what the flux? *Trends in Genetics*, 30(2):41 – 48, 2014.

[5] Magdalena Biedroń and Alicja Banasiak. Auxin-mediated regulation of vascular patterning in arabidopsis thaliana leaves. *Plant Cell Reports*, pages 1215–1229, 9 2018.

[6] Joshua J Blakeslee, Wendy A Peer, and Angus S Murphy. Auxin transport. *Current Opinion in Plant Biology*, 8(5):494 – 500, 2005. Cell signalling and gene regulation.

[7] Yoshinori Hayakawa, Masashi Tachikawa, and Atsushi Mochizuki. Mathematical study for the mechanism of vascular and spot patterns by auxin and pin dynamics in plant development. *Journal of Theoretical Biology*, 365:12 – 22, 2015.

[8] Rainer Hertel and Rand Flory. Auxin movement in corn coleoptiles. *Planta*, 82(2):123–144, 06 1968.

[9] R.M.H. Merks, Y. Van de Peer, D Inzé, and G.T.S. Beemster. Canalization without flux sensors: a traveling-wave hypothesis. *Trends in Plant Science*, 12(9):384 – 390, 2007.

[10] Adam Runions, Richard S. Smith, and Przemyslaw Prusinkiewicz. Computational models of auxin-driven development. pages 315–357, 2014.

[11] T. SACHS. Polarity and the induction of organized vascular tissues. *Annals of Botany*, 33(2):263–275, 03 1969.

[12] Michael Sauer, Stéphanie Robert, and Jürgen Kleine-Vehn. Auxin: simply complicated. *Journal of Experimental Botany*, 64(9):2565–2577, 05 2013.

[13] Klaartje van Berkel, Rob J. de Boer, Ben Scheres, and Kirsten ten Tusscher. Polar auxin transport: models and mechanisms. *Development*, 140(11):2253–2268, 2013.

[14] J. Van der Voort. The travelling wave movement of the auxin hormone. 2019.

[15] Yidong Wang, Tao Zhang, Rongchen Wang, and Yunde Zhao. Recent advances in auxin research in rice and their implications for crop improvement. *Journal of Experimental Botany*, 69(2):255–263, 07 2017.

[16] Dolf Weijers and Doris Wagner. Transcriptional responses to the auxin hormone. *Annual Review of Plant Biology*, 67(1):539–574, 2016. PMID: 26905654.

[17] Beatrix Zaban, Wenwen Liu, Xingyu Jiang, and Peter Nick. Plant cells use auxin efflux to explore geometry. *Scientific Reports*, 4(1):5852, Jul 2014.

Appendix A

Appendix

A.1 The simulation with fixed initial Auxin

```
%Timerange
tRange=[0,100];

%Amount of cells
n=100;

%Initial conditions
Z0 = zeros(1,4*n+2);
%Setting start value
Z0(1)=1;

%Executing the solver
[tSol,ZSol]=ode45(@ODEsystem,tRange,Z0);

%%
function dZdt = ODEsystem(t,Z);
    %Setting Parameters
    n=100;
    Tact=800;
    TdiffLab=0.15;
    ka=1;
    R=100;
    kR=100;
    k1=2;
    k2=5*10^(-3);
    km=100;
    alpha=0.1;
    Δ=0.0001;
    lambda = 0.5;
    h= 1000;
    phi=1;
    theta=0;


```

```
35      Auxine = zeros(1,n+1);
36      Proteine = zeros(1,n+1);
37      RProteine = zeros(1,n);
38      LProteine = zeros(1,n);
39
40      Auxineterm = zeros(1,n+1);
41      Proteineterm = zeros(1,n+1);
42      Activation = zeros(1,n+1);
43
44      Afgeleide = zeros(1,4*n+2);
45
46      for i = 1:4*n+2
47          if (i < n+2)
48              Auxine(i)=Z(i);
49              Auxineterm(i)= Auxine(i)/(ka+Auxine(i));
50              Activation(i)=Auxine(i) * R / (kR + Auxine(i));
51          elseif (i < 2*n + 3 && i > n + 1)
52              Proteine(i-n-1)=Z(i);
53              Proteineterm(i-n-1)=Proteine(i-n-1)/(km+Proteine(i-n-1));
54          elseif i < 3*n+3
55              RProteine(i-2*n-2)=Z(i);
56          elseif i < 4*n+3
57              LProteine(i-3*n-2)=Z(i);
58          end
59      end
60
61      J = zeros(1,n);
62      for i = 1:n
63          J(i) = ...
                phi*(Auxine(i)*RProteine(i)-Auxine(i+1)*LProteine(i));
64      end
65
66      H= zeros(2,n+1);
67      H(1,1) = (1/(1+exp(-h*(J(1)/lambda-theta))))
68      /((1/(1+exp(-h*(J(1)/lambda-theta))))+(1/(1+exp(h*theta))));
69      H(2,1) = (1/(1+exp(h*theta)))
70      /((1/(1+exp(-h*(J(1)/lambda-theta))))+(1/(1+exp(h*theta))));
71      for i = 2:n
72          H(1,i) = (1/(1+exp(-h*(J(i)/lambda-theta))))
73          /((1/(1+exp(-h*(J(i)/lambda-theta))))
74          +(1/(1+exp(-h*(-J(i-1)/lambda-theta)))));
75          H(2,i) = (1/(1+exp(-h*(-J(i-1)/lambda-theta))))
76          /((1/(1+exp(-h*(J(i)/lambda-theta))))
77          +(1/(1+exp(-h*(-J(i-1)/lambda-theta)))));
78      end
79      H(1,n+1)=0;
80      H(2,n+1)=0;
81
82      Afgeleide(1) = ...
            Tact*(LProteine(1)*Auxineterm(2)-RProteine(1)*Auxineterm(1))
83      +TdiffLab*(Auxine(2)-Auxine(1));
84      for i = 2:n-1
85          Afgeleide(i) = Tact*(RProteine(i-1)*Auxineterm(i-1)
86          +LProteine(i)*Auxineterm(i+1)
87          -(LProteine(i-1)+RProteine(i))*Auxineterm(i))
88          +TdiffLab*(Auxine(i+1)+Auxine(i-1)-2*Auxine(i));
89      end
```

```
90      Afgeleide(n) = Tact*(RProteine(n-1)*Auxineterm(n-1)
91      -(LProteine(n-1)+RProteine(n))*Auxineterm(n))
92      +TdiffLab*(Auxine(n-1)-2*Auxine(n));
93      Afgeleide(n+1) ...
            =Tact*(RProteine(n)*Auxineterm(n))+TdiffLab*(Auxine(n));
94
95      Afgeleide(n+2)= -lambda*Proteine(1)*(H(1,1)) + ...
            k2*(RProteine(1))+alpha*Auxine(1)-Δ*Proteine(1);
96      for i = 2:n
97          Afgeleide(i+n+1)= -lambda*Proteine(i) + ...
                k2*(RProteine(i)+LProteine(i-1))
98          +alpha*Auxine(i)-Δ*Proteine(i);
99      end
100     Afgeleide(2*n+2) = 0;
101
102     Afgeleide(2*n+3)= lambda*Proteine(1)*H(1,1)-k2*RProteine(1);
103     Afgeleide(3*n+3)= lambda*Proteine(2)*H(2,2)-k2*LProteine(1);
104     for i = 2:n-1
105         Afgeleide(i+2*n+2)= ...
                lambda*Proteine(i)*H(1,i)-k2*RProteine(i);
106         Afgeleide(i+3*n+2)= ...
                lambda*Proteine(i+1)*H(2,i+1)-k2*LProteine(i);
107     end
108     Afgeleide(3*n+2)= lambda*Proteine(n)*H(1,n)-k2*RProteine(n);
109     Afgeleide(4*n+2)= 0;
110
111     dZdt= [Afgeleide]';
112 end
```

A.2 Generating data by running the simulation

```
1  tic;
2  fileID = fopen('Golfdata (Aux,PIN,RPIN,LPIN), ...
       (0.01,0.01,1,1500).txt','w'); %Opening datafile
3  fprintf(fileID,'\n','Maximum','Speed','Golfbreedte');
4
5  for i = 1:1:10 %Running the simulation
6      FluxmodelV4(i,1500)
7  end
8
9  %Importind data from datafile
10 Temp= importdata("Golfdata (Aux,PIN,RPIN,LPIN), ...
       (0.01,0.01,1,1500).txt");
11 Golfdata = Temp(:,:);
12 GPiek = Golfdata(:,1);
13 GSnelheid = 1./Golfdata(:,2);
14 GBreedte = Golfdata(:,3).*(1./Golfdata(:,2));
15 PinPiek = Golfdata(:,4);
16 PinSnelheid = 1./Golfdata(:,5);
17 PinBreedte = Golfdata(:,6).*(1./Golfdata(:,5));
18 RPinPiek = Golfdata(:,7);
19 RPinSnelheid = 1./Golfdata(:,8);
20 RPinBreedte = Golfdata(:,9).*(1./Golfdata(:,8));
```

```
21 LPinPiek = Golfdata(:,10);
22 LPinSnelheid = 1./Golfdata(:,11);
23 LPinBreedte = Golfdata(:,12).*(1./Golfdata(:,11));
24
25
26
27 toc;
```

A.3 Rescaling Auxin waves

```
1  tic;
2
3
4  hold on
5  for j = 0.01:0.01:0.1
6      FluxmodelV4(j,3000);
7      AUX=importdata('AUXdata.txt'); %tSol en ZSol of cell 50 ...
           being imported from FluxmodelV4
8      Prop=importdata('AUXdata2.txt'); %The maximum, speed, width ...
           and time of maximum of Auxin in cell 50
9      AUXine = zeros(1, length(AUX(:,1)));
10
11     for i = 1:length(AUX(:,1))
12         AUXine(i) = AUX(i,2)/Prop(1); %Scaling wave in height
13     end
14     AUXine(Prop(4)) = AUX(Prop(4),2)/Prop(1);
15
16
17     if j == 0.01
18         plot((AUX(:,1)-AUX(Prop(4),1))/Prop(3)+50,AUXine,
19         'Linewidth', 2) %Plotting the first line a bit thicker
20     end
21     plot((AUX(:,1)-AUX(Prop(4),1))/Prop(3)+50,AUXine, ...
           'Linewidth', 1) %Scaling wave in width
22     xlim([49.5, 52])
23     xlabel('Time')
24     ylabel('Normalized Auxin concentration')
25
26 end
27 hold off
28 legend('0.01','0.02','0.03','0.04','0.05','0.06','0.07','0.08',
29 '0.09','0.1')
30
31 toc;
```

A.4 The simulation with constant Auxin influx

```
1
2  % function FluxmodelV5_Pulsjes(Meettijd)
```

```
3
4  %Timerange
5  tRange=[0,200];
6
7  %Amount of cells
8  n=60;
9
10 %Initial conditions
11 Z0 = zeros(1,4*n+2);
12 %Instellen van beginwaarden
13 Z0(1)=0;
14
15 %Executing the solver
16 [tSol,ZSol]=ode45(@ODEsystem,tRange,Z0);
17
18 %Auxine per cel, 1 t/m n+1
19 Z1 = ZSol(:,1:n);
20 plot(tSol,Z1)
21 xlabel('Tijd')
22 ylabel('Auxin in cell 1 t/m n+1')
23 legend('Cell1', 'Cell 2', 'etc')
24
25 plot(tSol,ZSol(:,60))
26 xlabel('Time')
27 ylabel('Auxin-concentration')
28 legend('Cell 60')
29
30
31 %Calculate peak
32 a=findpeaks(ZSol(:,60));
33 c=ZSol(:,60);
34 TF=islocalmin(c);
35
36 interval = zeros(1,19);
37 j=1;
38 tSol(TF);
39 for i=1:length(tSol)
40     if TF(i)==1
41         i;
42         interval(j)=i;
43         j=j+1;
44     end
45 end
46
47 clear pieken
48 clear WaveSojournTime
49
50 for i = 1:18
51     clear tempSol
52     clear tempZSol
53     clear tijd
54
55     tempSol = tSol(interval(i):interval(i+1));
56     tempZSol(:,60) = ZSol(interval(i):interval(i+1),60);
57
58     a=max(tempZSol(:,60));
59     index(1,i) = find(tempZSol(:,60) ≥ 0.05*a, 1, 'first');
```

```
60      index(2,i) =find(tempZSol(:,60) ≥ 0.05*a, 1, 'last');
61
62      for j=1:2
63          tijd(j) = tempSol(index(j,i));
64      end
65
66      interval(i);
67      pieken(i) = a;
68      WaveSojournTime(i) = tijd(2)-tijd(1);
69  end
70
71  for i = 1:length(pieken)
72      % Writing peak and wave sojourn time to file
73      fileID = fopen('PiekVSBreedte.txt','a');
74      fprintf(fileID,'%f %f \n', pieken(i), WaveSojournTime(i))
75  end
76
77  scatter(pieken, WaveSojournTime)
78  xlabel('Wave Amplitude')
79  ylabel('Wave Sojourn Time')
80  legend('Een golf in meerdere paketten')
81
82
83  function dZdt = ODEsystem(t,Z);
84      %Setting Parameters
85      n=60;
86      Tact=800;
87      TdiffLab=0.15;
88      ka=1;
89      R=100;
90      kR=100;
91      k1=2;
92      k2=1.5*10^(-1);
93      km=100;
94      alpha=0.1;
95      ∆=1.0;
96      lambda = 0.5;
97      h= 900;
98      phi=1;
99      theta=0.01;
100
101
102     Auxine = zeros(1,n+1);
103     Proteine = zeros(1,n+1);
104     RProteine = zeros(1,n);
105     LProteine = zeros(1,n);
106
107     Auxineterm = zeros(1,n+1);
108     Proteineterm = zeros(1,n+1);
109     Activation = zeros(1,n+1);
110
111     Afgeleide = zeros(1,4*n+2);
112
113     for i = 1:4*n+2
114         if (i < n+2)
115             Auxine(i)=Z(i);
116             Auxineterm(i)= Auxine(i)/(ka+Auxine(i));
```

```
117             Activation(i)=Auxine(i) * R / (kR + Auxine(i));
118         elseif (i < 2*n + 3 && i > n + 1)
119             Proteine(i-n-1)=Z(i);
120             Proteineterm(i-n-1)=Proteine(i-n-1)/(km+Proteine(i-n-1));
121         elseif i < 3*n+3
122             RProteine(i-2*n-2)=Z(i);
123         elseif i < 4*n+3
124             LProteine(i-3*n-2)=Z(i);
125         end
126     end
127
128     J = zeros(1,n);
129     for i = 1:n
130         J(i) = ...
                phi*(Auxine(i)*RProteine(i)-Auxine(i+1)*LProteine(i));
131     end
132
133     H= zeros(2,n+1);
134     H(1,1) = (1/(1+exp(-h*(J(1)/lambda-theta))))
135     /((1/(1+exp(-h*(J(1)/lambda-theta))))+(1/(1+exp(h*theta))));
136     H(2,1) = (1/(1+exp(h*theta)))
137     /((1/(1+exp(-h*(J(1)/lambda-theta))))+(1/(1+exp(h*theta))));
138     for i = 2:n
139         H(1,i) = (1/(1+exp(-h*(J(i)/lambda-theta))))
140         /((1/(1+exp(-h*(J(i)/lambda-theta))))
141         +(1/(1+exp(-h*(-J(i-1)/lambda-theta)))));
142         H(2,i) = (1/(1+exp(-h*(-J(i-1)/lambda-theta))))
143         /((1/(1+exp(-h*(J(i)/lambda-theta))))
144         +(1/(1+exp(-h*(-J(i-1)/lambda-theta)))));
145     end
146     H(1,n+1)=0;
147     H(2,n+1)=0;
148
149     Afgeleide(1) = ...
            Tact*(LProteine(1)*Auxineterm(2)-RProteine(1)*Auxineterm(1))
150     +TdiffLab*(Auxine(2)-Auxine(1))+0.1;
151     for i = 2:n-1
152         Afgeleide(i) = Tact*(RProteine(i-1)*Auxineterm(i-1)
153         +LProteine(i)*Auxineterm(i+1)
154         -(LProteine(i-1)+RProteine(i))*Auxineterm(i))
155         +TdiffLab*(Auxine(i+1)+Auxine(i-1)-2*Auxine(i));
156     end
157     Afgeleide(n) = Tact*(RProteine(n-1)*Auxineterm(n-1)
158     -(LProteine(n-1)+RProteine(n))*Auxineterm(n))
159     +TdiffLab*(Auxine(n-1)-2*Auxine(n));
160     Afgeleide(n+1) ...
            =Tact*(RProteine(n)*Auxineterm(n))+TdiffLab*(Auxine(n));
161
162     Afgeleide(n+2)= -lambda*Proteine(1)*(H(1,1)) + ...
            k2*(RProteine(1))+alpha*Auxine(1)-Δ*Proteine(1);
163     for i = 2:n
164         Afgeleide(i+n+1)= -lambda*Proteine(i) + ...
                k2*(RProteine(i)+LProteine(i-1))
165         +alpha*Auxine(i)-Δ*Proteine(i);
166     end
167     Afgeleide(2*n+2) = 0;
168
```

```
169       Afgeleide(2*n+3)= lambda*Proteine(1)*H(1,1)-k2*RProteine(1);
170       Afgeleide(3*n+3)= lambda*Proteine(2)*H(2,2)-k2*LProteine(1);
171       for i = 2:n-1
172           Afgeleide(i+2*n+2)= ...
                  lambda*Proteine(i)*H(1,i)-k2*RProteine(i);
173           Afgeleide(i+3*n+2)= ...
                  lambda*Proteine(i+1)*H(2,i+1)-k2*LProteine(i);
174       end
175       Afgeleide(3*n+2)= lambda*Proteine(n)*H(1,n)-k2*RProteine(n);
176       Afgeleide(4*n+2)= 0;
177
178       dZdt= [Afgeleide]';
179   end
```